

Review

Acyclic Nucleic Acids with Phosphodiester Linkages—Synthesis, Properties and Potential Applications

Agnieszka Tomaszewska-Antczak *  and Piotr Guga 

Centre of Molecular and Macromolecular Studies, Polish Academy of Sciences, Sienkiewicza 112,
90-363 Lodz, Poland; pguga@cbmm.lodz.pl

* Correspondence: atom@cbmm.lodz.pl; Tel.: +48-(42)-6803215

Abstract: This review summarizes the synthetic efforts on acyclic analogs of nucleic acids and provides information on the most interesting features of selected classes of such compounds. The selection includes the following types of analogs: Flexible (FNA), Unlocked (UNA), Glycol (GNA), Butyl (BuNA), Threoninol (TNA) and Serinol Nucleic Acids (SNA). These classes of analogs are discussed in terms of their synthetic methods, the thermal stability of their homo- and hetero-duplexes and their applicability in biological and biochemical research and nanotechnology.

Keywords: acyclic nucleic acids; stability of nucleic acid complexes; fluorescent nucleic acid probes; siRNA



Citation: Tomaszewska-Antczak, A.; Guga, P. Acyclic Nucleic Acids with Phosphodiester Linkages—Synthesis, Properties and Potential Applications. *Appl. Sci.* **2021**, *11*, 12125. <https://doi.org/10.3390/app112412125>

Academic Editors: Michal Sobkowski, Adam Kraszewski and Joanna Romanowska

Received: 29 October 2021

Accepted: 15 December 2021

Published: 20 December 2021

Publisher's Note: MDPI stays neutral with regard to jurisdictional claims in published maps and institutional affiliations.



Copyright: © 2021 by the authors. Licensee MDPI, Basel, Switzerland. This article is an open access article distributed under the terms and conditions of the Creative Commons Attribution (CC BY) license (<https://creativecommons.org/licenses/by/4.0/>).

1. Introduction

The abbreviations DNA and RNA are perhaps the most widely recognized words associated with biology or genetics. The details of their chemical structure as well as the principles of their interactions with other nucleic acids were established in the 20th century, but modern analytical methods developed in recent years allow the study of their still poorly understood subtle interactions with other biomolecules. On the other hand, significant advances in organic and analytical chemistry have led to the synthesis of numerous DNA and RNA analogs that can be used as biochemical probes or drugs. To target DNA or RNA in cells, these analogs must not only cross outer cell membranes and form stable complexes with the target molecules in a sequence-specific manner, but they should also have some resistance to nucleases in body fluids. The beneficial use of multiple COVID-19 vaccines is a very compelling example of the importance of nucleic acid analogs to billions of people.

A single nucleotide unit consists of three segments that are chemically very different from each other. The heterocyclic nucleobases serve as acceptors and donors of hydrogen bonds and are responsible for proper intermolecular recognition. In addition, stacking interactions are important in conferring a high degree of rigidity to oligomers and higher-order structures. The anionic phosphodiester groups are reasonably stable under mild hydrolytic conditions, but they are important for hydration and may be involved in electrostatic interactions with positively charged amino acid side chains and other cationic species. Not to be neglected is the electrostatic repulsion between the phosphate moieties present in the oligonucleotide chains forming a complex, which contribute to the rigidity of the entire DNA or RNA system. The third component comprises of sugar moieties (ribose or 2'-deoxyribose), which are present in the cyclic form. Notably, the pseudo-rotational flexibility of the ribonucleotide is considerably limited due to the anomeric effect, and RNA/RNA and RNA/DNA duplexes are generally more thermally stable than DNA/DNA duplexes. The rigidity of the cyclic scaffold has been considered important for the formation of thermally stable duplexes [1], and the unexpectedly high thermal stability of duplexes formed with the participation of LNA oligomers could serve as an excellent justification for this point of view. However, this generalization is not consistent with the behavior

of Peptide Nucleic Acids (PNA), in which the heterocyclic bases are attached to a linear peptide-like backbone, since duplexes composed of RNA or DNA and PNA strands are far more stable than RNA/RNA and DNA/DNA ones. This phenomenon may be attributed to the absence of a negative charge in the backbone, such that the absence of repulsive interactions balances the entropic cost of proper spatial organization of the flexible PNA scaffolds. Nonetheless, the widely accepted importance of the cyclic sugar components for the stability of the duplexes could be questioned. There is another perspective that can be applied to the acyclic analogs of nucleic acids that is related to the origin of life. We are currently witnessing an ongoing dispute about which molecule, DNA or RNA, was the first to mark the beginning of life in its modern form, i.e., were the first carriers of the contemporary genetic information. However, even if the correct answer is finally found, there is still the question of its possible predecessors. The first suggestion that oligomers with an acyclic flexible scaffold carrying pro-chiral nucleotide analogs might play such a role was made in 1987 by Joyce et al. [2]. These flexible structures seemed to be easier to produce than deoxyribo- or ribo-nucleosides under prebiotic conditions. To assess the possibility of their involvement in, for example, primer extension experiments, which could be considered the simplest biochemical probe showing a “living-like” system, chemists had to make several model compounds. Thus, both perspectives triggered efforts to synthesize and evaluate numerous acyclic analogs of nucleic acids, and it must be admitted that in several cases, very astonishing properties were found. They may be used not only in biochemical probes but, perhaps in the somewhat distant future, also in medicine and outside biology, e.g., in nanoelectronics. This review aims to summarize these synthetic efforts and to provide information on the most interesting properties of selected classes of such compounds. The selection includes the following types of analogs:

- Flexible Nucleic Acids (FNA)
- Unlocked Nucleic Acids (UNA)
- Glycol Nucleic Acids (GNA)
- Butyl Nucleic Acids (BuNA)
- Threoninol Nucleic Acids (TNA)
- Serinol Nucleic Acids (SNA)

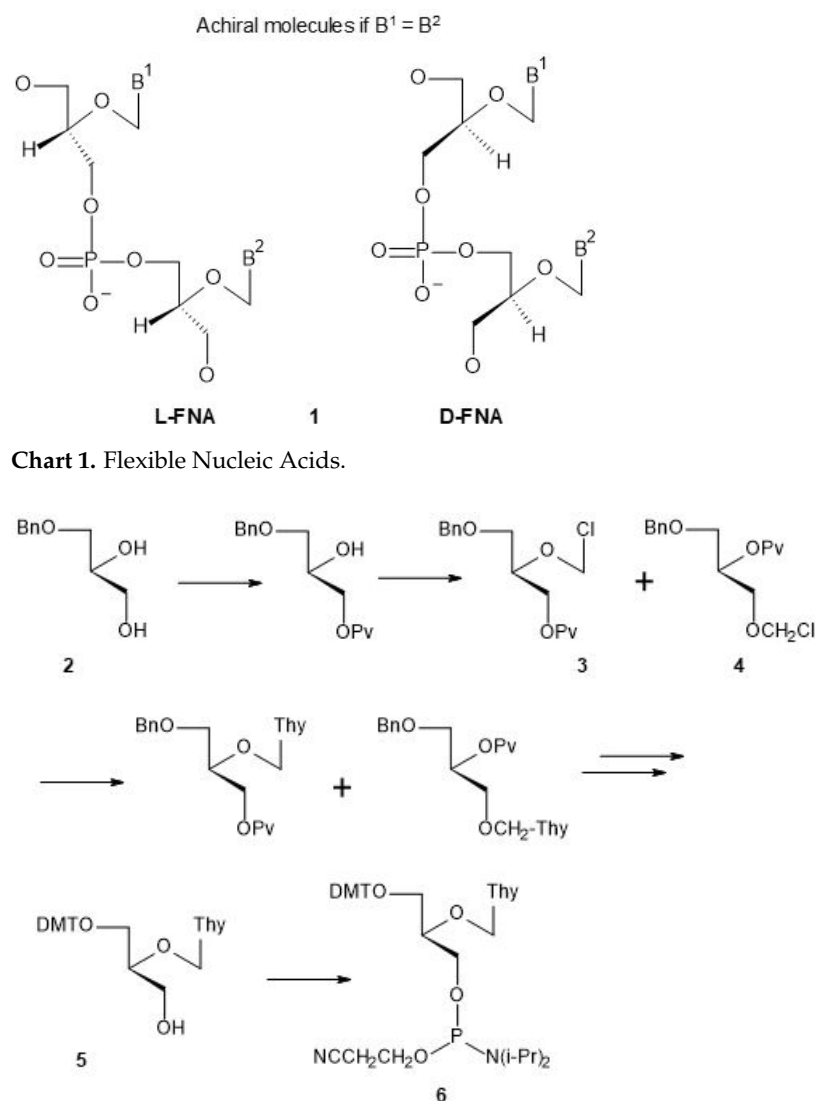
These analogs are presented and discussed in terms of their synthetic methods, thermal stability of their homo- and hetero-duplexes, their applicability in biological and biochemical research and nanotechnology.

2. Flexible Nucleic Acids (FNA)

Flexible Nucleic Acids (FNA, **1**, Chart 1, shown are dinucleotides) were one of the first proposed acyclic nucleotides for an evolutionary precursor to DNA and RNA, and were the first synthesized acyclic analogs of DNA. Since FNA are deprived of the 2'-carbon atom, that is otherwise part of the relatively rigid D-ribose ring present in the nucleosides of DNA or RNA series, their structural flexibility is virtually unrestricted. Only the anionic phosphate moieties provide some repulsive forces of the electrostatic nature, which work against the stacking interactions caused by the nucleobases. This first synthesis of the FNA-related acyclic nucleoside was reported by Schneider and Benner [3]. The multistep synthesis (Scheme 1) began with a 1-O-benzyl derivative of glycerol.

While glycerol itself is an achiral molecule, any derivatization at either of the two primary hydroxyl groups leads to a chiral compound producing L-FNA or D-FNA depending on the chiral glycerol derivative used in the synthesis. The Swiss researchers used (S)-1-O-benzyl glycerol (**2**), but due to the O3→O2 migration of the pivaloyl protecting group during the chloromethylation of **2**, a mixture of two regioisomers (**3** + **4**, in the ratio 2:1) was formed. Substitution of thymine for the chlorine atoms in **3** and **4**, followed by removal of the benzyl group, dimethoxytritylation and removal of the pivaloyl group, afforded the desired compound **5** and its regioisomer. They were separated chromatographically and **5** was routinely converted to the phosphoramidite monomer **6**, which was used in the solid phase synthesis of oligomers of the general sequences 5'-d(CTTTTTTTG)-3'

and 5'-d(CAAATAAAG)-3'. These oligomers consisted mainly of DNA, with the FNA unit at position 4 or two FNA units at positions 4,6 or 4,5. A 13-mer 5'-d(CtttttttG)-3' ("t" stands for the FNA-T unit) was also obtained. Interestingly, in the synthesis of these oligomers, the coupling yields were approximately 90% for **6** and >99% for standard DNA phosphoramidite monomers. The DMT-tagged oligonucleotide products were isolated by RP-HPLC and then detritylated. The resultant oligomers were hydrolyzed with spleen phosphodiesterase, snake venom phosphodiesterase (svPDE) and dephosphorylated with bacterial alkaline phosphatase, giving the mixtures containing the expected nucleosides in the expected ratios.



Scheme 1. Synthesis of the FNA-T phosphoramidite monomer.

It was found that the oligomers containing 1 or 2 FNA-T units destabilized the (FNA-DNA)/DNA duplexes by about 15 °C per modification, compared to $T_m = 40$ °C found for the natural DNA. The almost completely modified oligomer d(CtttttttG) did not form a duplex with the complementary 5'-d(GAAAAAAAAAAC)-3'. Destabilization was attributed to an increase in entropy cost compared to the perfect duplex formed by natural nucleic acids. Pure oligothymidylate and oligoadenylate FNA and their alternating copolymers (12–19 mers) were synthesized by Merle and collaborators [4]. Interestingly, using the same phosphoramidite method, the repetitive yield of +98% was observed, while subsequent thermal dissociation studies showed that (FNA-A)₁₂ hybridized effectively with dodecathymidylate (dT)₁₂ and the complex exhibited sharp melting with $T_m = 24$ °C.

Rather unexpectedly, although DNA/DNA duplexes adopt a B-type conformation, the circular dichroism (CD) spectrum suggested that the FNA/DNA duplex exists as an A-type helix, as is the case for RNA/RNA or RNA/DNA duplexes. Some differences were observed during svPDE-assisted hydrolysis, because while $t_{1/2} = 38$ s was found for T_{12} , for the oligomers FNA- A_{12} and alternate FNA-(A(A-T) $_9$), the values were 110 h and about 12 h, respectively. It should be emphasized that there are no classical 3' and 5' ends in fully modified FNA oligomers, since both ends are chemically equivalent, allowing the enzyme to start hydrolysis from either end.

Chaput and Switzer studied the nonenzymatic oligomerization reaction on hairpin templates containing several FNA-C units, which was considered a model for studying prebiotic replication of informational macromolecules [5]. It was found that the acyclic FNA-C units effectively attracted guanosine 5'-phosphoro-2-methylimidazole molecules and did not block the template-directed oligomerization. PAGE Analysis performed after 10 days showed elongation by up to 7 nucleotides.

3. Unlocked Nucleic Acids (UNA)

In 1995, Wengel and collaborators described the synthesis of DNA oligonucleotides with 1–3 acyclic unlocked thymidine nucleotides (7, Chart 2, B=Thy, a dinucleotide is shown), that have an OH group at the 2' position, yet lack a covalent bond between the 2' and 3' carbon atoms [6]. The synthesis of the relevant UNA nucleoside (Scheme 2) was based on the oxidative cleavage of the vicinal diol in 5'-O-DMT-protected 2'-hydroxythymidine (8, B=Thy), followed by a reduction of the resultant dialdehyde 9 with sodium borohydride.

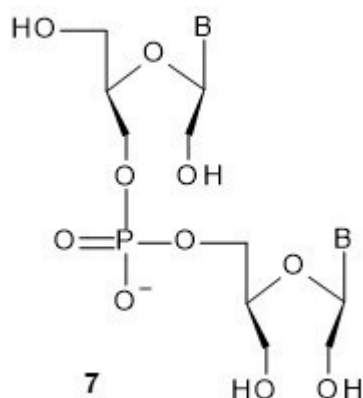
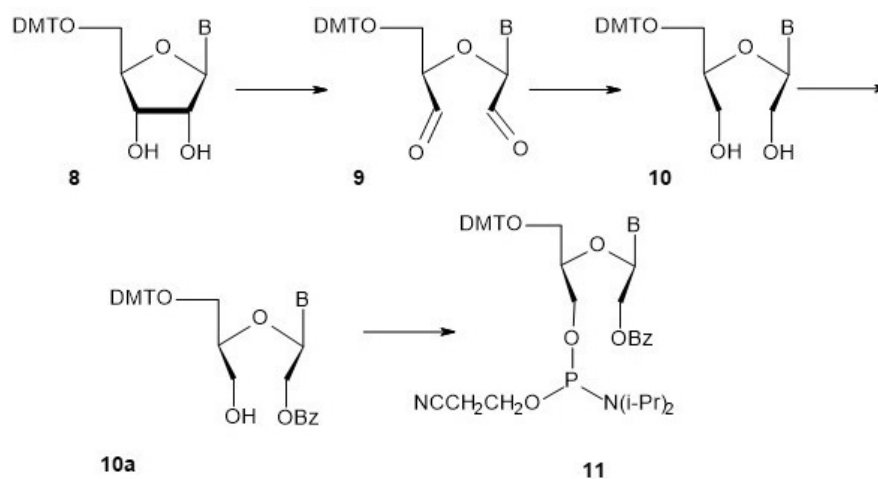


Chart 2. Structure of UNA dinucleotide.



Scheme 2. Synthesis of the phosphoramidite derivative of a UNA nucleoside.

The unlocked nucleoside **10** (obtained in 88% yield) was then benzoylated, but the desired 2'-O-Bz compound (**10a**, isolated in 38% yield) was accompanied by the 3'-O-Bz regioisomer (17%). After routine phosphitylation of **10a**, the required phosphoramidite monomer **11** (B=Thy) was obtained in good yield and used in the automated solid-phase synthesis of the above-mentioned oligomers. In 2009, the synthesis of other UNA-nucleosides **10** was published and good yields were reported (B=A^{Bz}: 73%, C^{Ac}: 64%, G^{iBu}: 63%, U: 79%) [7]. The benzoylated derivatives **10a** were obtained in 63–79% yields. The synthetic route to UNA was improved by the synthesis of 2'-O-TBDMS monomers [8].

A biocatalytic route for the regioselective preparation of the benzoyl derivative should also be mentioned [9]. In this approach, for the selective benzoylation of 2'-hydroxyl function in 5'-O-DMT-2',3'-seco-uridine (**10**, B=Ura) with vinyl benzoate, five lipases, i.e., *Candida Antarctica* lipase-B, *Thermomyces lanuginosus* lipase, *Amano* PS lipase, *Candida rugose* lipase and porcine pancreatic lipase, were tested in five organic solvents. *Thermomyces lanuginosus* lipase was found to induce selective and efficient benzoylation in toluene, yielding the desired product **10a** (in 92% yield), which was then successfully converted to the corresponding phosphoramidite monomer **11** (B=Ura).

These monomers were used in the automated solid phase synthesis of chimeric DNA-UNA and RNA-UNA oligomers. Further studies showed that the UNA units confer them remarkably high stability in serum [7,10].

A single UNA nucleotide present in a DNA strand decreases the T_m value for the corresponding (UNA-DNA)/DNA duplex by 10 °C [6]. The thermal stability of RNA/DNA and RNA/RNA duplexes containing one or two UNA nucleotides, as well as the effects of mismatches, were investigated using a set of 8 RNA 21-mers of a general sequence 5'-UGCACUGUAUGUCUGUACCAU-3' and 5'-ACUUGUGGCCAUUUACGUCGC-3' [7]. It was found that for duplexes formed with DNA or RNA templates, a single UNA unit in a central position of the RNA strands lowered T_m values by 5–8 °C. When the mismatches were positioned directly opposite a UNA monomer, only little discrimination was observed. Additionally, two UNA monomers can be used to decrease or increase mismatch discrimination depending on their position in the oligomers. This phenomenon was used to detect a breast cancer onco micro-RNA (miR-10b) and distinguish it from two other miRNAs (miR-10a and miR10c) that differed from miR10b by one and two nucleotides, respectively [11]. A fluorescently labeled 5'-(FAM)-CACAAATTCGGTTCTACAGGGTA-3' with 2 UNA units (underlined) used in combination with water-soluble nano-graphene oxide proved to be 50 times more effective than the fully complementary DNA probe.

The CD spectra indicate that a UNA nucleotide can be considered structurally as an RNA mimic, since the incorporation of one or a few UNA monomers into the RNA/RNA duplexes does not change the overall structure compared to that of the unmodified duplex, which is important for biochemical applications [12]. However, UNA nucleotides located close to the center of the oligomer make the corresponding RNA duplex structure 4.0–6.6 kcal/mol less favorable. Much smaller destabilization (0.5–1.5 kcal/mol) is caused by UNA residues located near the 5' or 3' ends. Thermodynamic analysis of a large set of UNA-modified oligomers showed that UNA pyrimidine nucleotides cause greater destabilization than purine nucleotides, and the thermodynamic effects of the UNA substitutions are additive. It was also documented that UNA nucleotides interact according to the Watson-Crick base-pairing rules, while the stacking interactions of UNA nucleotides are less favorable than those of RNA units.

The UNA nucleotides have also been studied in terms of their effects on the stability of other high-ordered structures, i.e., *i*-motif and G-quadruplex. It is known that C-rich oligonucleotides can adopt *i*-motif structures, in which the rigid core is formed due to intercalation of C-C⁺ base pairs present in a single strand or in a complex of up to four strands, possibly arranged in a few orientations [13]. Such fragments have been found in biologically important structures and appear to be important in the regulation of biological processes. A widely known *i*-motif sequence is a 22-nt fragment of human telomeric DNA with the sequence 5'-d(CCCTAA)₃CCCT). This molecule was engineered to form twelve

22-nt oligomers, each containing a single UNA modification located in oligomers in a “walking mode” [14]. The thermodynamic stability of the *i*-motif structures was measured in buffers of pH 4.8 and 5.6. It was found that the UNA units, depending on their position, either destabilize (positions C1 or C14) or stabilize (U10, A11, A12) the structure. The recorded CD spectra allow to conclude that the UNA-nucleotides do not cause significant changes in the *i*-motif structure and folding molecularity.

The G-quadruplexes are formed from G-rich nucleic acid fragments and their characteristic feature is a stack of planar G-quartets interacting according to the Hoogsteen scheme of hydrogen bonding. The quartets can be formed by guanosine nucleotides present in a single strand or in a complex of up to four strands, and are stabilized by several cations, in particular by potassium and sodium ions. Generally, K⁺ cations stabilize guanine-quartet assemblies to a larger extent than Na⁺. It is well-documented that G-quadruplexes are capable of tuning many biological processes. The influence of UNA nucleotides on the structure and stability of G-quadruplexes was investigated using CD spectroscopy, as G-quadruplexes generate unique CD signals. After analyzing a series of oligomers of the general sequence GGGTTTTGGGA(T,C)GGTTTTGGG, it was found that UNA nucleotides present in the loops cause global stabilization of the structure, while those in the stem cause destabilization of the quadruplexes [15]. These observations were relevant to the study of the UNA-modified thrombin-binding aptamer 5'-GGTTGGTGTGGTTGG-3', which forms an intramolecular antiparallel G-quadruplex that interacts with two thrombin molecules and inactivates only one of them. Again, a library of fifteen modified oligomers containing UNA nucleotides (distributed in a “walking mode”) was prepared, and UV melting analysis was applied to obtain thermodynamic parameters as well as information on the stoichiometry of the folding process [16]. These studies revealed remarkable destabilization of the quadruplexes when UNA-G nucleotides were located in the segments forming the G-quadruplex structure. Substitutions of UNA-U for U were much less disruptive. Considering the ΔG°_{37} for the quadruplex formation, the UNA-U units introduced at positions 3, 7 or 12 make quadruplex folding more energetically favorable than when observed with the unmodified aptamer. The inhibitory effect of the aptamer analogs on blood clotting time was measured using a standard thrombin time assay. It was found that an aptamer analog carrying UNA-U at position 7 (a loop position) inhibited blood clotting more than the unmodified compound. This research was continued with the UNA-2'-C-(piperazin-N-yl)-U moiety, in which the piperazine unit is protonated under physiological conditions [17]. This modification was chosen due to reports in the literature that this derivative destabilizes DNA and DNA/RNA duplexes less than regular UNA monomers [10]. A single 2'-C-(piperazin-N-yl)-UNA residue or 2–3 UNA residues were incorporated at positions 3, 7 or 12 (*vide supra*) of the aptamer and the thermodynamics, kinetics and biological properties were evaluated. It was found that the UNA unit with the piperazine tag provided more efficient stabilization of the quadruplex compared to regular UNA (by 0.28–0.44 kcal/mol) in a position-dependent manner, with retained quadruplex topology and molecularity. However, this generally had a negative effect on binding affinity and biological activity, with the exception of those at position 7, as the binding affinity and inhibitory properties were comparable to those of the unmodified aptamer. Finally, a UNA moiety modified within a nucleobase was tested, namely a 4-thiouracil (^{S4}U) derivative [18]. As in the previous experiments, the most favorable thermodynamic parameters were obtained by introducing the UNA-^{S4}U nucleotide at positions 3, 7 or 12, although similar effects were observed for the RNA-^{S4}U unit. Introduction of UNA-3'-deoxy-3'-amino-U at the above-mentioned key positions 3, 7 or 12 (the phosphate group was attached at the 2'-O oxygen atom) decreased the thermal denaturation temperature of the tetraplex by 4–7 °C and reduced thrombin clotting times by 32–42 s, compared with the unmodified aptamer (87 s) [19]. Considering a literature report showing that 2'-deoxy-isoguanosine at positions 1, 8 or 10 in the thrombin-binding aptamer enhances the aptamer–thrombin interaction [20], Pasternak and co-workers prepared 14 aptamer analogs carrying the RNA-

or UNA-type isoguanine derivative, but all proved to be poor anticoagulants compared to the unmodified aptamer [21].

Pasternak and co-workers also studied an RE31 aptamer, which is a longer version of the thrombin-binding aptamer 5'-GGTTGGTGTGGTGG-3' mentioned above. RE31 is a 31-nt oligomer (originally developed by Mazurov and co-workers [22]) consisting of the G-quadruplex and a duplex domain linked by four nucleotides. The 15-nt G-quadruplex parts are identical in both aptamers, whereas the duplex domain of RE31 consists of six pairs of complementary nucleotides. Of the 13 analogs synthesized, 6 oligomers contained a single UNA unit (A, C, G and U), one oligomer had 3 UNA nucleotides, other compounds contained one UNA and multiple LNA nucleotides and one oligomer was modified with 14 β -L-RNA units [23]. The greatest increase in thermal stability of RE31 was observed for oligomers labeled with the LNA units present in the duplex fragment or with a combination of LNAs in the helix and UNAs at position 15. Additionally, ternary substitution of T11, T15 and T20 by UNA-U resulted in a 5.4 °C increase in T_m . Only a minor stabilizing effect was observed for the other aptamers. Structural studies confirmed that the overall shape of RE31 analogs remained unchanged and that all analyzed aptamers formed antiparallel G-quadruplexes at 37 °C. All analyzed analogs of RE31 possessed prolonged biological stability in human serum.

Several papers have been published on the use of UNA nucleotides to improve the potency of siRNA oligomers. Typically, siRNA oligomers are RNA duplexes of 21 base pairs containing a 19-mer base-pairing stem and 2-nt 3'-overhangs. The discovery of their ability to knock down gene function has made significant progress in mammalian cell culture studies. However, unmodified siRNAs suffer from insufficient selectivity of the gene regulatory process and limited stability in body fluids. Therefore, the use of UNA nucleotides seemed to be at least a partial solution to these problems. Indeed, some siRNAs with UNA units proved to be remarkably stable (e.g., in mice) and, in contrast to unmodified siRNAs, they efficiently induced knock-down of eGFP expression in a pancreas tumor xenograft model [24]. However, the great complexity of the RNAi mechanism confronts researchers with many factors that must be considered to properly identify the effects of UNA-nucleotides and other chemical modifications on siRNA activity [25–28].

UNA-nucleotides have also been tested as fluorescently labeled compounds to be used as sensitive probes in molecular biology or nanotechnology. Two pyrene-modified UNA monomers were synthesized and incorporated into 21-mer DNA oligonucleotides [29]. Pyrene is a widely used chromophore due to its long fluorescence lifetime, high sensitivity and ability to stabilize DNA duplexes. The reported units differed in a linker between the 2'-(piperazin-N-yl) moiety and the pyrene molecule, which was either an amide (**12**, X=O, Chart 3) or an alkylamine (**12**, X=H,H). It was found that both pyrene-UNA-U units increased the duplex stability compared to UNA monomers, although the corresponding unmodified reference duplexes were still the most stable. Thermodynamic studies showed that they were able to discriminate mismatches well. Pyrene excimer emission was observed in single-stranded oligonucleotides containing three pyrene-UNA-U units, which disappeared after hybridization with DNA. Interestingly, for the first time, the fluorescence intensities of oligomers containing acyclic pyrene-nucleotides were found to increase upon hybridization with DNA or RNA templates. The unit containing the alkylamino linker (**12**, X=H,H) was used to construct a quencher-free molecular beacon that showed an increase in pyrene excimer emission of more than 900% upon hybridization of a fully complementary RNA target. This probe enabled the detection of RNA in H1299 cells [30]. Two additional pyrene-labeled UNA-U were synthesized using 5'-O-DMT-5-iodo-uridine (**13**, Scheme 3), which was converted to regioisomeric UNA-5-(pyren-1-yl)-U (**14** and **15**) after cleavage of the C2'-C3' bond. These compounds were converted into corresponding 3'-O- and 2'-O-phosphoramidite monomers suitable for the formation of 3'-5'- and 2'-5'-internucleotide bonds, respectively [31]. Both units were found to destabilize *i*-motif structures at pH 5.2. Moreover, their presence in a DNA strand resulted in reduced thermal stability of duplexes formed with DNA and RNA strands, although to a lesser extent than with

unmodified UNA monomers. In addition, a bis-pyrene-labeled UNA-U was synthesized (**16**, Chart 4) with one pyrene moiety attached to position 5 of the uracil and the other to the 2'-(piperazin-N-yl) fragment [32]. As with the mono-labeled compounds, the compound with two labels was found to decrease the thermal stability of both DNA/DNA and DNA/RNA duplexes, but the destabilization was less than in the case of the unmodified UNA monomers. This compound also exhibits high mismatch discrimination. The UV/Vis absorption and molecular modeling studies allowed to conclude that the pyrene units are localized in the major groove of a duplex and do not intercalate with the nucleobases.

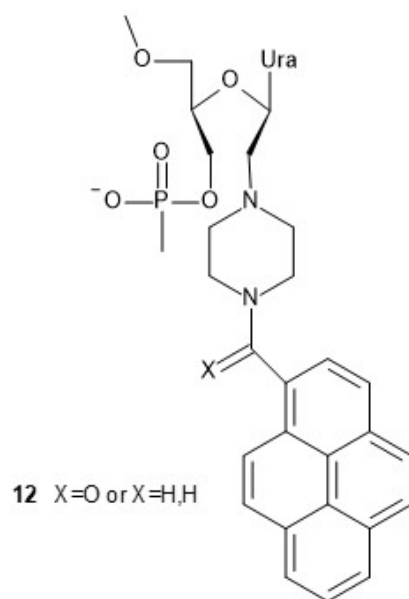
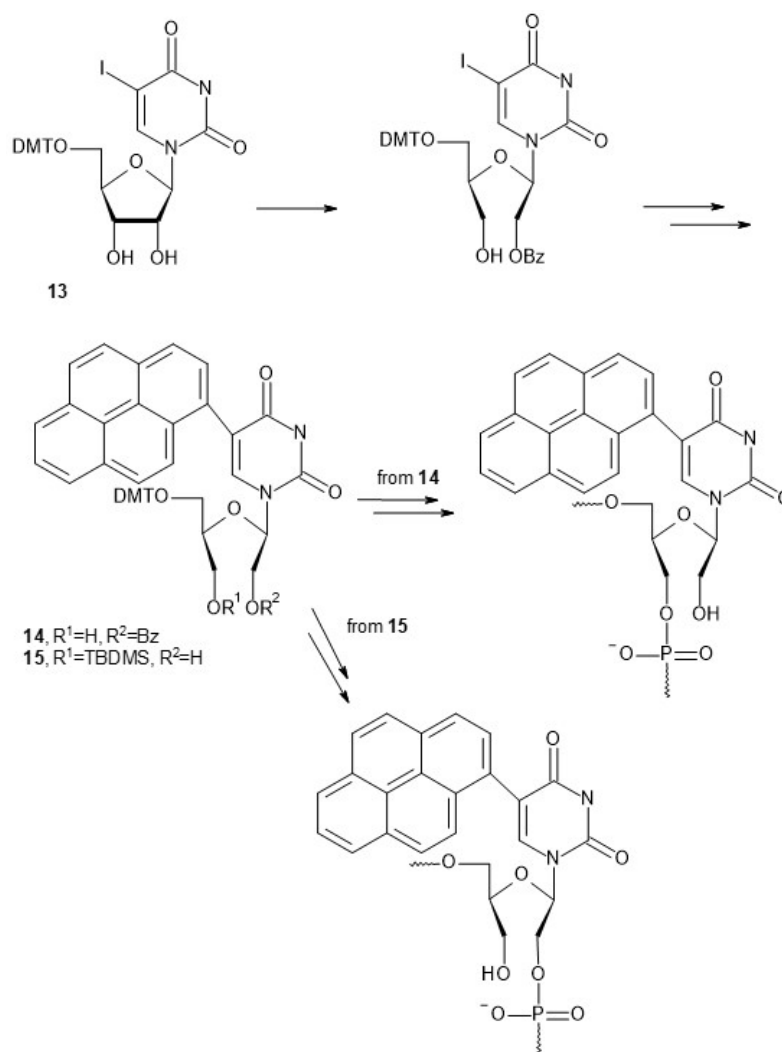


Chart 3. Pyrene-modified UNA nucleotide.

In the synthesis of a UNA-3'-O-amino-U nucleoside (**17**, Scheme 4; Note: **17** is not a 3'-deoxy-3'-amino compound), the previously developed synthon **10a** (B=Ura) was used [33]. Its labeling with pyrene and the standard conversion of the resultant UNA-(5'-O-DMT- 3'-O-amino-pyrene)-U (**18**) into a phosphoramidite monomer allowed the preparation of oligomers containing this fluorescent pyrene probe. Thermal dissociation studies showed that the presence of UNA-(3'-O-amino-pyrene)-U in DNA or 2'-OMe RNA oligomers (21-nt long) resulted in increased thermal stability of duplexes with a DNA complement. Fluorescence spectroscopy studies indicated that the pyrenes were located in the minor grooves of the duplexes, and these results were confirmed by molecular modeling, CD, and UV/Vis absorption experiments. Pyrene-pyrene excimer signals were observed for oligomers bearing two or three pyrene-labeled units. Upon hybridization with the complementary DNA strand, the excimer signals disappeared, allowing such constructs to be used for fluorescence-based detection of mismatched hybridization. It was also found that the UNA-(3'-O-amino-pyrene)-U unit stabilizes triplexes under mildly acidic conditions and fluorescence emission was observed only at temperatures above the melting point of the triplex. Thus, the modification may help to detect triplex-forming double-stranded DNA sequences.



Scheme 3. Synthetic route to two regioisomers of pyrene-labeled UNA-U derivatives suitable to form 3'-5' or 2'-5' inter-nucleotide bonds.

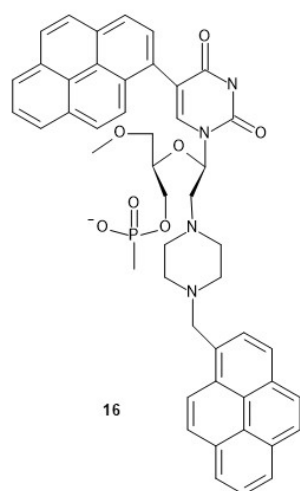
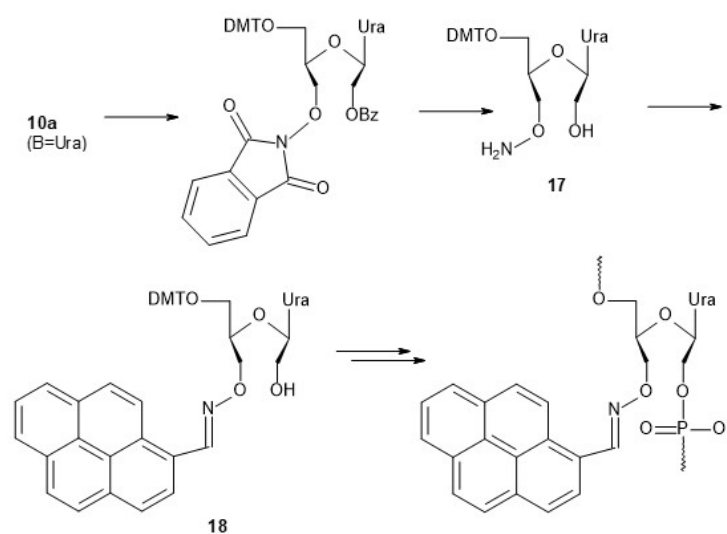


Chart 4. Bis-pyrene-labeled UNA-U.



Scheme 4. Synthetic route to oligomers with UNA-(3'-O-amino-pyrene)-U units.

4. Glycol and Butyl Nucleic Acids (GNA and BuNA)

Structurally simple and synthetically relatively easily accessible acyclic glycol nucleic acids (GNA; **19**, Chart 5, B=Thy or Ade, a dinucleotide is shown) were obtained by Meggers and coworkers in 2004 and reported in 2005 [34]. Note that unlike FNA and UNA, a GNA scaffold contains stereogenic centers (marked with the asterisks in **19**) and GNA units can exist in *R* and *S* forms. Fortunately, the enantiomerically pure substrates, i.e., (*S*)-(-)-glycidol (**20**, Chart 5) and (*R*)-(+)-glycidol (**21**), are commercially available. After dimethoxytritylation, the DMT derivatives were successfully ring-opened with the unprotected thymine and adenine. The adenine derivative was benzoylated at the exocyclic amino group, and the product and thymine derivative were converted into the final phosphoramidities, which were further used in the solid-phase synthesis of 7 oligomers, each 18-nt in length. Their sequences allowed the study of the formation of antiparallel and parallel duplexes. It was found that uniformly modified GNA oligomers form highly stable ($T_m = 63\text{ }^\circ\text{C}$) antiparallel helical duplex structures according to the Watson-Crick base-pairing scheme. This stability significantly exceeds the thermal stability of the analogous DNA duplex. The recorded melting curves showed a characteristic sigmoidal shape, while the curves of the oligomers intended to form a parallel duplex showed no transition. Notably, a single mismatch in the middle of the sequence significantly reduced the stability of the duplex ($T_m = 55\text{ }^\circ\text{C}$). It was found that (*S*)-GNA and its Watson-Crick-paired (*R*)-GNA counterpart neither hybridize with each other nor form stable duplexes with DNA. However, initial results showed that (*S*)-GNA 2'-ATTTTAAATATAATAATT-3' (and not (*R*)-GNA) associates with RNA ($T_m = 35\text{ }^\circ\text{C}$).

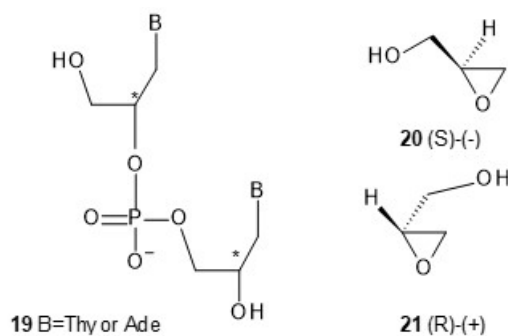


Chart 5. GNA dinucleotide and enantiomers of glycidol.

The GNA derivatives of cytosine, guanine and uracil were prepared in a similar manner, although to obtain the guanine derivative, the reaction of 2-amino-6-chloropurine

had to be used, followed by hydrolysis with 1N HCl [35]. The ring opening yields of 49–61% were only satisfactory. The crystal structures of the glycol nucleosides confirmed the formation of the desired regioisomers. The syntheses of the corresponding phosphoramidite monomers were rather routine and it was shown that GNA oligonucleotides can be synthesized in high yield under the conditions of solid-phase synthesis. Analysis of the thermal stability of a GNA/GNA duplex formed by 3'-CACATTATTGTTGTA-2' with 2'-GTGTAATAACAACAT-3' revealed a T_m of 71 °C compared to 46 °C for a normal DNA duplex of the same sequence. The CD spectrum recorded for this duplex showed greatly increased CD signals at around 205, 220, and 275 nm, supporting the formation of a helical duplex.

Based on long-term observations, it was found that the widely used amide protecting groups in the monomers used for solid-phase synthesis of GNA lead to the formation of by-products, resulting in lower final yields than expected. In addition, the GNA-G phosphoramidite is unstable and decomposes slowly, even at –20 °C. To alleviate these problems, an N-dimethylformamidinium protecting group was chosen for adenine and guanine and an acetamide group for cytosine [36]. The new phosphoramidite derivative of GNA-G^{dmf} proved to be stable when chromatographed on a silica gel column, and the monomer was obtained in a significantly higher yield (30% vs. 8%). Using these new monomers, several GNA oligonucleotides were prepared following the general procedures for the synthesis of DNA oligonucleotides, except that the coupling time of 3 min was applied. Cleavage from the solid support and deprotection of the exocyclic amino protecting groups was carried out in 15–20 min at 55 °C using a 1:1 mixture of 40% aqueous methylamine and 25% aqueous ammonium hydroxide. The RP-HPLC analysis confirmed a much higher quality of the crude oligonucleotide product compared to the previous method.

Further studies showed that even a single GNA nucleotide incorporated in the middle of the DNA oligomer strongly destabilized the corresponding (GNA-DNA)/DNA duplex [37]. For example, for 5'-CACATTA(S-T^{GNA})TGTT and its (R-T^{GNA}) counterpart mixed with 3'-GTGTAATAACAACAT-5', the T_m values were 13 and 7 °C lower, respectively. Three glycol nucleotides in the 15-mer DNA strand further decrease the stability of the corresponding (GNA-DNA)/DNA duplex to $T_m = 29$ °C. It was also found that (S)-GNA, but not (R)-GNA, hybridize well with RNA strands containing only A:T base pairs. Surprisingly, G:C base pairs lead to strong destabilization of these ((S)-GNA-RNA)/RNA duplexes.

To characterize the reasons for the high stability of certain GNA duplexes, the values of ΔG (Gibbs free energy), ΔH (change in enthalpy) and ΔS (change in entropy) for the formation of three duplexes were determined from melting experiments [38]. The calculated thermodynamic parameters indicate that the entropic toll for GNA is much lower than that for DNA, so there must be a strong conformational preorganization of the GNA strands. There were also other results indicating particularly favorable stacking interactions in GNA duplexes. However, whereas in B-DNA the base–base stacking interactions predominantly operate in an intra-strand fashion, in GNA duplexes, these energetically beneficial contacts are between the bases of the opposite strands. These conclusions were strongly supported by the results of X-ray analysis of the (S)-GNA duplex formed by the self-complementary 3'-CGHATHCG-2', where the H nucleotide contains the artificial hydroxypyridone nucleobase, which forms a highly stable H:H pair in the presence of copper(II) ions. These two Cu²⁺-binding pockets allowed the introduction of two heavy atoms per duplex to help for phasing the crystallographic data [39]. The analysis confirmed the extensive inter-strand base–base stacking interactions. The right-handed (S)-GNA double helix differs markedly from the canonical A- and B-form nucleic acid helices. A large helical pitch of 60 Å (34 Å for DNA and RNA) with 16 residues per turn (10 and 12 for DNA and RNA, respectively) and a large helical rise (3.8 Å vs. 3.4 Å and 2.9 Å) were also observed. The base pairs are displaced from the helix axis (x-displacement) by 5.1 to 8.6 Å. The authors describe the GNA helix structure as “a helical ribbon loosely wrapped around the helix axis”. How-

ever, X-ray analysis of the 3'-G(⁵BrC)GCGC oligomer yielded markedly different results. Here, all nucleobases form standard Watson-Crick hydrogen-bonding patterns and the 5-bromocytosine nucleotide had virtually no distorting effect. In this duplex, a helical pitch of 26 Å and 10 base pairs per turn were observed [40]. The differences have been explained by the fact that in the metallo-GNA duplex structure, all standard nucleotides adopt a *gauche* conformation with respect to the torsional angles between C2'-O and C3'-O, whereas the hydroxypyridone glycol nucleotides adopt *anti* conformations. These two forms of backbone conformation, an elongated M-type (containing metallo-base pairs) and the condensed N-type (containing brominated base pairs), were further analyzed using molecular dynamics (MD) simulations over a period of 20 ns [41]. The calculations also utilized data collected for a new crystal of a GNA duplex (with a resolution of 1.8 Å—it belongs to the condensed N-type) obtained from the self-complementary GNA 3'-CTC(⁵BrU)AGAG-2'. All bases form standard Watson-Crick hydrogen bonds, with the negligible distortion effect coming from the presence of the 5-bromouracil nucleotides. The MD simulations of dsGNA explained the high thermal stability of the duplex by a combination of enthalpic and entropic factors, but also revealed a pronounced "twisting/untwisting" behavior of the dsGNA backbone. This feature can significantly complicate the design of GNA probes intended for sequence-specific recognition.

In the field of molecular biology, GNA oligomers have been tested as templates for template-dependent synthesis of DNA using the polymerases Taq, Bst, DeepVent (exo-), Terminator, Sequenase and SuperScript II DNA [42]. The chances of success were not good because GNA and DNA oligomers do not form stable duplexes. The DNA primer (5'-TAATACGACTCACTATAGGG-3') was labeled at the 5' end with ³²P-phosphate and annealed to a DNA-GNA chimeric templates 3'-ATTATGCTGAGTGATATCCCatatcag-5', or 3'-ATTATGCTGAGTGATATCCCDtDtcDgcDgtcA-5', where lowercase letters denote GNA nucleotides and "D" stands for a diaminopurine nucleotide (see structure 36). For most polymerases, the primer extension process stalled after elongation of the primer by two or three deoxynucleotides. However, the Bst DNA polymerase catalyzed full-length DNA synthesis on a dodecamer GNA template. In another study, the ability of various DNA polymerases (*vide supra*) to use GNA triphosphates as substrates for GNA synthesis on DNA templates was investigated [43]. It was found that the Terminator DNA polymerase was able to extend the primer by incorporating two GNA units, whereas extension with up to five GNA nucleotides was much less efficient. Some improvement was achieved by using 5-propynyl-substituted GNA-C, where the propynyl substituent was assumed to enhance stacking interactions. This assumption was incorrect for a GNA-(5-propynyl-T) nucleotide.

In another type of experiment, a GNA-T unit was introduced into a molecule of the thrombin-binding aptamer mentioned above, the important part of which is a G-quadruplex [44]. The GNA-T nucleotide was introduced at position 3, 4, 7, 9, 12 or 13, and in all cases, these substitutions decreased the melting temperature (by approximately 10 °C), except at position 7, where T_m increased by 5 °C. However, no data were shown on the effects of these substitutions on the activity of the aptamer. The effect of GNA substitution on the potency of the siRNA probe was also investigated. First, the effect of incorporation of (S)- or (R)-GNA nucleotides on the RNA duplex structure was investigated using three individual crystal structures [45]. It was found that the (S)-GNA nucleotide backbone adopts a near-neutral conformation for the overall duplex structure, while the (R)-nucleotide dislocates the phosphate backbone and alters the hydrogen bonding of an adjacent base pair. Modification of an siRNA with (S)-GNA resulted in higher *in vitro* efficacy than analogs with (R)-GNA. Notably, duplexes modified with GNA were able to maintain their efficacy *in vivo* when injected subcutaneously into mice.

For potential applications in molecular biology, sufficient resistance to light-induced damage is an important factor. Therefore, it is promising information that regardless of the absolute configuration of the GNA-T units, GNA-TT dinucleotides are not photo-crosslinked in aqueous solution [46]. Samples were exposed to 254 nm radiation for 3 h. UV

spectra showed no significant change in UV absorbance around 270 and 330 nm, indicating that the thymine chromophore remained intact. This resistance was explained by a small overlap interaction between adjacent thymine residues. After such irradiation, the reference TpT dinucleotide lost 50% of its absorbance at 270 nm.

Several reports indicate a potential application of GNA oligomers in nanotechnology. Since GNA provides easy access to both left- and right-handed helical geometries, these molecules can potentially be used to construct nanostructures with unique topologies. Chapat and co-workers published a report on the synthesis of two 4-helix junctions (4HJ) with mirror-image symmetry using (*R*)- or (*S*)-GNA monomers [47]. The CD spectra for both GNA 4HJ nanostructures were similar to previous CD data collected on double-stranded GNA duplexes. This indicates that short helices were present in each arm of the 4HJ. However, the spectra differed significantly from spectra typical of natural DNA and RNA helices, suggesting that the GNA helices have a unique helical structure. Melting experiments showed that the GNA 4HJ was significantly more stable than the corresponding DNA 4HJ (76 vs. 37 °C).

The aforementioned artificial hydroxypyridone nucleobase and C6-(pyridin-2-yl)purine, acting as either homo- or hetero-base pairs, were introduced into a GNA duplex 3'-AATATTAXTATTTTA-2'/2'-TTATAATYATAAAAT-3' and tested for their ability to accommodate a range of metal cations [48]. For all three combinations of base pairs, the addition of CuSO₄ and NiCl₂ resulted in a huge increase (by 18–37 °C) in the thermal stability of the duplexes, compared to the same GNA duplex in the absence of the transition metal salt. These duplexes were also significantly more stable than the reference duplex with X=A and Y=T. Smaller effects were found for AgNO₃, Co(NO₃)₂ and ZnCl₂, and the effects for Pd(NO₃)₂ and AuCl₃ were negligible. The authors suggested that such metallo-GNAs can be used for the generation of duplexes with interesting electronic and magnetic properties.

Metal-dependent tuning of the thermal stability of GNA duplexes was found for GNA nucleotides with diphenylporphyrinacetylide (**R**, **22**, Chart 6) [49].

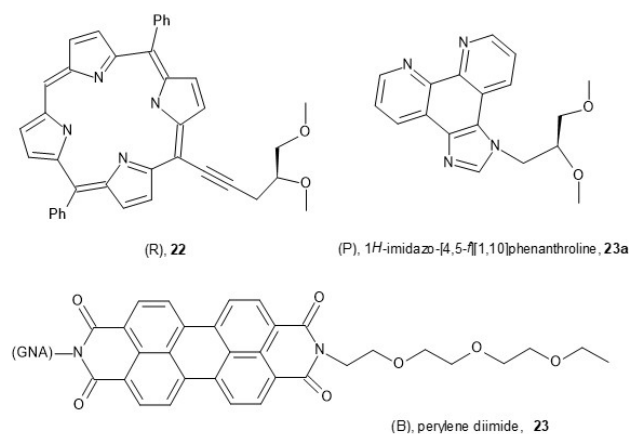


Chart 6. GNA nucleotides labeled with fluorophores.

When the porphyrin acetylide-labeled GNA unit (**R**) is incorporated opposite an abasic ethylene glycol site (**H**), the resultant duplexes, e.g.,



or



are thermally destabilized, but the overall structures of the GNA duplexes remain very little changed. Interestingly, the thermal stabilities of such **R:H** base pairs can be modulated by the addition of Zn²⁺ and Ni²⁺, as these cations decrease and increase the

duplex stability, respectively. Such porphyrin-GNA conjugates can potentially be used for light collection and charge transport.

A stabilizing effect ($\Delta T_m = 10\text{ }^\circ\text{C}$) of electrostatic complementarity between the electron-deficient perylene diimide (B, **23**, Chart 6) and the relatively electron-rich porphyrin (R), which serve as the nucleobases in the middle of the 16-mer GNA duplex 3'-TAAAAATHR $\underline{\text{TAAT}}$ ATT-2' / 2'-ATTTTTABHATTATAA-3' (H stands for the abasic site), has been reported [50]. However, while 2, 4 or 5 consecutive chromophores (arranged in a zipper-like inter-strand alternating fashion) provided an approximately cumulative effect ($\Delta T_m = 16\text{--}25\text{ }^\circ\text{C}$), only $\Delta T_m = 3\text{ }^\circ\text{C}$ was observed for a set HRH/BHB.

Several experiments were performed with GNA units located within DNA oligomers and carrying unnatural nucleobases. A GNA nucleoside analog containing 1*H*-imidazo[4,5-*f*][1,10]phenanthroline (P, **23a**, Chart 6) as a nucleobase was found to form a base pair within a DNA duplex 5'-d(GAGGGTPTGAAAG)-3' / 3'-d(CTCCCAPACTTTC)-5', which was able to coordinate a Cu⁺ cation, with a marked increase in T_m (+23 °C) [51]. Unmodified duplexes with A:T or G:C base pairs in place of the P:P base pair did not respond to the presence of this cation. Importantly, this probe was insensitive to Cu²⁺ cations for geometric reasons, leading to some repulsion effects. This differentiation can be used to tune a duplex dissociation/association process by changes in the redox state of the copper cation.

The same authors reported that the addition of 2 equivalents of Zn²⁺ to a duplex:

5'-d(AAAAAAAAAAPTAATTTTTPAATATTT)-3'

3'-d(TTTTTTTTTTPATAAAAPTTATAAA)-5' resulted in a 9 °C increase in duplex T_m [52].

Using a similar model:

5'-d(AAAAAAAAAATTAATTTTTAATATTT)-3'

3'-d(TTTTTTTTTTPATAAAAPTTATAAA)-5',

with two base pairs P:T, it was shown that at a pH of 5.5, after the addition of 2 equivalents of Hg²⁺, the stability of the duplex increased significantly ($\Delta T_m = 14\text{ }^\circ\text{C}$) [53]. Interestingly, using the slightly modified duplex:

5'-d(AAAAAAAAAAPTAATTTTTPAATATTT)-3' /

3'-d(TTTTTTTTTTCATAAAATTTATAAA)-5'

it was possible to selectively load one modified base pair (P:T) with Hg²⁺ and the other (P:C) with Ag⁺. A similar phenomenon was observed for a duplex 5'-d(GAGGGAPAGAAAG)-3' / 3'-d(CTCCCTPTCTTTC)-5' (a P:P base pair), where $\Delta T_m = 4.3\text{ }^\circ\text{C}$ was observed after addition of the Hg²⁺ cation, although $\Delta T_m = 14.5\text{ }^\circ\text{C}$ was observed for a P:T base pair [54].

More recently, Kowalski and coworkers published the synthesis of a ferrocenyl-labeled analog of the nucleoside GNA-U (GNA-FcU, **24**, Chart 7) [55]. Cyclic voltammetry studies of a chimeric dinucleoside phosphate (GNA-FcU)p(rA_{2',3'-O,O}-isopropylidene) revealed the presence of a one-electron ferrocenyl-centered redox wave. A half-wave potential of 99 mV against the FcH/FcH⁺ couple was found. The authors suggest a future application of GNA-FcU in the synthesis of redox-active self-assembling "molecular wires".

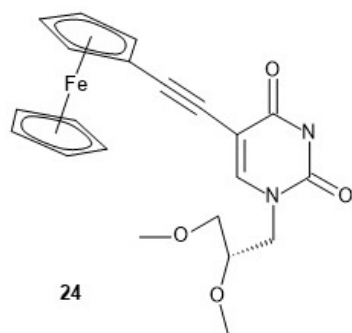


Chart 7. Ferrocenyl-labeled analog of the nucleoside GNA-U.

Apart from the acyclic structure, GNA nucleotides differ from DNA and RNA units in the number of atoms present in the backbone units. There are 5 atoms in GNA (O3'-C3'-C2'-O2'-P) and six atoms in natural nucleotides (O5'-C5'-C4'-C3'-O3'-P). It has been suggested that the difference in linker length is one reason why GNA oligomers do not hybridize with DNA. Therefore, it was tempting to make a homolog of GNA with six atoms in the backbone, and this was carried out with the synthesis of Butyl Nucleic Acids (BuNA, **25**, Chart 8) [56]. In the first attempt, the carboxyl groups of (*S*)-malic acid were reduced to yield the corresponding triol, in which two hydroxyl groups were protected using benzaldehyde dimethyl acetal. Then, the nucleobases were substituted for the third hydroxyl under the conditions of a Mitsunobu reaction. By this synthetic route, the intermediates bearing uracil, thymine and adenine were obtained in 40–60% yield, but the further workup was successful only for the uracil derivative, so the relevant scheme is not shown. The BuNA derivatives of Ade, Thy, Gua and Cyt were obtained starting from aspartic acid (**26**, Scheme 5), which was subjected to NH₂ → Br conversion (using an HNO₂/HBr mixture), followed by a reduction of the carboxyl groups and epoxide ring closure.

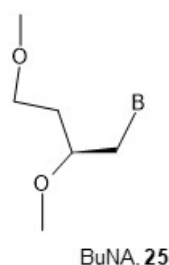
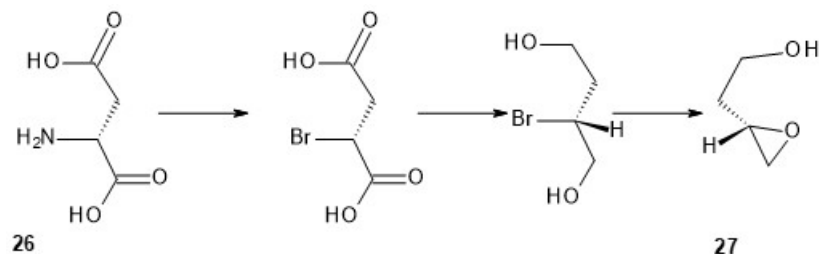


Chart 8. Structure of BuNA nucleotide.



Scheme 5. Synthesis of the epoxyalcohol substrate for synthesis of BuNA nucleosides.

The resulting epoxy alcohol **27** was tritylated with DMT-Cl and reacted with thymine, benzoylated cytosine, adenine or 2-amino-6-chloropurine. It should be noted that starting from one enantiomer of aspartic acid, only single enantiomers of BuNA nucleosides were obtained. Finally, after the protection of adenine and the conversion of 2-amino-6-chloropurine into guanine, the corresponding phosphoramidite monomers were obtained in good yield. Ten fully modified (eight of them with a DNA nucleoside at the 3'-end) and eight partially modified oligomers were synthesized. It was found that (*S*)-butyl nucleic acids (BuNA) form duplexes with their complementary strands, but the observed thermal stability was lower than that for corresponding DNA duplexes. Thus, increasing the backbone length by one carbon atom resulted in a decrease in the melting temperature of (*S*)-BuNA duplexes compared to GNA duplexes. Moreover, the CD spectra showed that (*S*)-BuNA duplexes adopt the A-like conformation and form a left-handed helical structure. The incorporation of (*S*)-BuNA nucleotides into DNA strands resulted in destabilized duplexes. The primer extension studies on fully modified (*S*)-BuNA strands and (*S*)-BuNA-substituted DNA were carried out using the polymerases Bst, Bsu, Taq and Terminator. No extension was observed with fully modified primers, but when (*S*)-BuNA-substituted DNA strands were used, full extension of the modified primers was observed.

5. Threoninol Nucleic Acids (TNA)

The nucleoside precursors of acyclic threoninol nucleic acid (D-aTNA, **28**, Chart 9, a dinucleotide is shown) were prepared using DMT-protected D-threoninol (**29**, Scheme 6), except for the thymine derivative, for which unprotected D-threoninol **30** was used [57]. The amino groups were used to attach N1-carboxymethyl derivatives of the nucleobases C^{Bz} or T, or N9-carboxymethyl derivatives of A^{Bz} or G^{iBu} under conditions known from peptide chemistry. The product containing a thymine nucleobase was tritylated and all four DMT-protected nucleosides **31** were routinely phosphitylated to yield the corresponding D-aTNA monomers **32**.

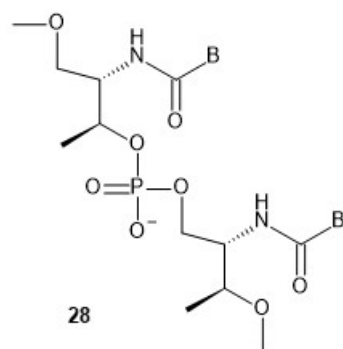
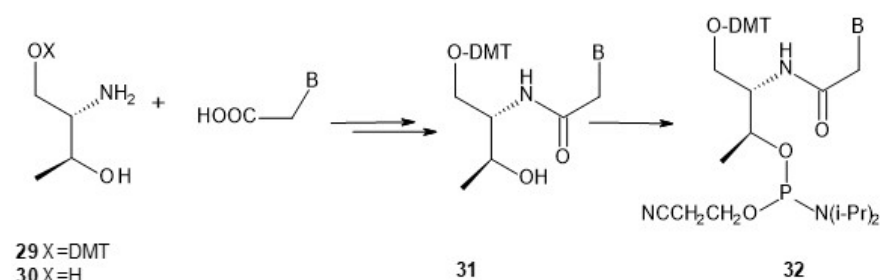


Chart 9. Structure of TNA dinucleotide.



Scheme 6. Synthesis of D-aTNA monomers **32**.

Using the monomers **32**, seven oligomers (each 8-nt long) were synthesized on an automated DNA synthesizer. The coupling efficiency of the TNA monomers was as high as that of the conventional monomers, as judged from the Vis absorption of the released DMT⁺ cation. After the recommended workup, the oligomers were purified by RP-HPLC and characterized by MALDI-TOF MS. Melting experiments showed that the D-aTNA oligomers 1'-GCATCAGT-3' and 3'-CGTAGTCA-1' formed an unexpectedly stable antiparallel duplex with T_m = 63 °C, compared with analogous DNA and RNA duplexes with 29 and 39 °C, respectively. Notably, a single T:C mismatch significantly lowered the T_m to 49 °C. CD studies showed that single-stranded D-aTNA oligomers, unlike GNA, do not form a helical preorganized structure. The same group reported the synthesis of L-aTNA using an optimized method analogous to that used in the synthesis of D-aTNA [58]. As expected from the enantiomeric relationship between L- and D-aTNA, the L-aTNAs formed an antiparallel homo-duplex with the same melting temperature (58 °C) as the D-aTNA duplex of the same sequence. However, unlike D-aTNA, L-aTNA not only hybridized quite well with both DNA (T_m = 25–28 °C) and RNA (T_m = 38–41 °C), but the association also occurred in a parallel manner. The crystal structure of an L-aTNA/RNA duplex (3'-GCAGCAGC-1')/(5'-GCUGCU^{Br}GC-3') clearly shows right-handed helicity and a Watson-Crick base-pairing [59]. The N-type sugar pucker was found in the RNA strand of the duplex, which is usually observed in an A-type duplex.

While a CD experiment identified a single-stranded L-aTNA oligomer 5'-TTTTTTTTTT TTTTT-4'-dT-3' as a random coil, the homopurine 5'-AAAAAAAAAAAAAAAA-4'-dA-3'

showed a preorganized structure (CD-positive signals at 267 and 218 nm and negative bands at 247 and 203 nm) [60]. This observation was confirmed by a UV melting curve. It was also found that the homopyrimidine L-aTNA with the sequence 5'-TTTTTTTTTTTTTT-4'-dT-3' forms a highly stable triplex L-aTNA/DNA/L-aTNA with 5'-d(GATCCAAAAAAAAAAAAAAAAAG)-3' ($T_m = 82\text{ }^\circ\text{C}$). Similarly, 5'-TCTCTCTCTCTTTT-4'-dT-3' and 5'-AGAGAGAGAGAAAAA-3' form an L-aTNA/RNA/L-aTNA triplex with $T_m = 66\text{ }^\circ\text{C}$. With both DNA and RNA central strands, the most stable triplexes were obtained when one L-aTNA strand was associated in an anti-parallel orientation and the other L-aTNA strand was associated in a parallel orientation relative to the DNA or RNA strand. It was also shown that L-aTNA is able to block Bsu DNA polymerase by forming a triplex with the DNA template.

The triplex formation phenomenon has been used for reversible regulation of polymerase activity and protein expression [61]. It was found that a construct of two acyclic L-aTNA homopyrimidine segments (linked to a hexaethylene glycol linker) and DNA (directly linked to an L-aTNA segment) can bind DNA and RNA by forming a highly stable triplex structure. The L-aTNA clamp is released from the target by adding a release strand in a kind of strand displacement reaction. The clamp hybridizes efficiently to a specific template and in this way inhibits the activity of Bsu and T7 RNA polymerase. This polymerase activity is reactivated by the displacement of the clamp. The clamp has been successfully used in the regulation of luciferase expression by reversible binding to mRNA. Binding to a sequence in the double-stranded plasmid downregulated protein expression by 40%.

Exploration of higher-order structures formed by aTNAs continued and L-aTNA-based G-quadruplex structures were identified [62]. T_m values of 47, 70 and 51 $^\circ\text{C}$, respectively, were observed for the structures formed by L-aTNAs 5'-GGGGGGG-4'-dT-3', 5'-GGGGGGGGGGG-4'-dT-3' and 5'-GGGTTTGGGTTTGGGTTTGGG-4'-dT-3' in 10 mM phosphate buffer containing 100 mM KCl (pH 7.4), while either no melting or $T_m = 33$ and 37 $^\circ\text{C}$, respectively, were observed in deionized water. UV-melting, CD, electrophoretic mobility shift assay and fluorescence studies showed that both intermolecular and intramolecular G-quadruplex structures can exist, the latter being more stable. The same group showed that at low pH, cytosine segments in L-aTNA form structures that exhibit the features of the *i*-motif [63]. To study their formation and properties, six oligomers were synthesized containing 6–11 L-aTNA-C nucleosides in a row or the CCCC(T)₂₋₃ segments repeated 3 times. Melting experiments showed that a melting transition was observed for all strands at low pH (41–81 $^\circ\text{C}$, at pH 4). The T_m values decreased with increasing pH, so that at pH 6, T_m 's $\leq 40\text{ }^\circ\text{C}$ were observed and no transition occurred for one oligomer. The molecularity of the structures was confirmed by ESI-MS as the detection of [4M-5H]⁵⁻ and [4M-7H]⁷⁻ ions for C₆dT indicated the presence of an *i*-motif with four single strands. The *i*-motif structures were characterized by CD and fluorescence spectroscopy, and the latter method was applied to mono-pyrene and bis-pyrene-labeled oligonucleotide strands. At low pH, a remarkable quenching of monomeric and excimer fluorescence occurred in mono- and bis-pyrene-labeled aTNA strands. At pH greater than the apparent pK_a of the *i*-motif structures, the pyrene emission was detected, and excimer fluorescence was observed in strands containing two pyrene units. The pH-controlled switching of fluorescence and excimer activity provides a basis for the design of a pH-sensitive probe and for the development of pH-switching molecular devices.

L-Threoninol-modified RNA molecules were tested as siRNAs in the RNAi pathway. Two L-aTNA-T units were incorporated at the 3'-termini of the antisense and sense RNA strands of siRNA targeting the *Renilla* luciferase mRNA [64]. Initial RNAi experiments were performed in HeLa cells using four (unmodified and modified) double-stranded siRNAs with the general sequences TTAAAAAGAGGAAGAAGUCUA-5'/5'-UUUUUCUCCUUCUUCAGAUTT, where the underlined TT were either d(TT) or L-aTNA-(TT), or combinations thereof. It was found that all siRNAs were potent inhibitors whose gene silencing was characterized by picomolar IC₅₀ values. Moreover, the siRNA con-

taining L-aTNA-(TT) in the 3'-overhang of the antisense strand showed 30% higher gene silencing than the siRNA carrying two natural thymidine residues. Control experiments showed that HeLa cells transfected with the *scrambled* siRNA produced luminescence similar to the untreated cells. A time-course analysis of the siRNAs over five days showed that the siRNA containing two L-threoninol units at both 3'-ends exhibited higher gene silencing activity than the native siRNA from day 3. This duplex showed exceptional stability in human serum, with ~5% of the original siRNA still intact after 8 h, whereas the native congener was completely degraded after approximately 60 min of incubation. Furthermore, the absence of cytotoxicity of the L-threoninol modification was determined by the MTT assay. The siRNA containing L-aTNA-(TT) activates IL-1 β production less efficiently than the unmodified siRNA, so the L-threoninol-thymine monomer may potentially be used to attenuate the activation of the immune response.

The effects of mismatches and/or L-aTNA modifications on the silencing activity of siRNAs were examined using the siRNA targeting the *Renilla* luciferase mRNA (*vide supra*) and its analogs, with mismatches at positions 9/10 and 10/11 in the sense strand (TTAAAAAGAGGA¹⁰A⁹GAAGUCUA-5') and in the antisense strand (5'-UUUUUCUCCU¹⁰U¹¹CUUCAGAUTT), respectively. However, the L-aTNA-T unit was introduced only in the antisense strand [65]. It was found that the melting temperature of RNA duplexes containing mismatches facing L-aTNA-T decreased by less than 3 °C compared to the perfect siRNA containing the L-aTNA monomer. For an (L-aTNA-T)¹¹:G⁹ mismatch, ΔT_m of only 0.7 °C was observed, i.e., within the measurement error. This duplex also showed the silencing activity quite similar to the parent (L-aTNA-T)¹¹:A⁹ (IC₅₀ 26.5 vs. 20.2 pM). Both these values and that for (L-aTNA-T)¹¹:U⁹ (35.6 pM) were only 2–3-fold higher than the 9.6 pM measured for the native duplex. For mismatches (L-aTNA-T)¹⁰:(U,C)¹⁰, silencing activities ranged from 216 to 270 pM, while (L-aTNA-T)¹⁰:G¹⁰ was identically active to the mismatch-free (L-aTNA-T)¹⁰:A¹⁰ (110 pM). Mismatches within the RNA family resulted in IC₅₀ values of 15–30 pM.

In the field of analytical biochemistry, DNA probes containing 2–6 D-threoninol-based units with a perylene moiety attached (instead of a nucleobase) have been used in experiments for fluorescence monitoring of DNA [66]. In these probes, each perylene-containing unit is separated by natural nucleotides, and without a complementary substrate, the linear probe does not emit fluorescence due to the self-quenching. When hybridized to the target DNA (complementarity over 17-nt was designed), intercalation of each dye between the base pairs results in emission of strong fluorescence. The signal-to-noise ratio was as high as 180, and the response rate was significantly faster than that of a reference hairpin-forming molecular beacon. This methodology was extended to the detection of RNA in cell lysates [67]. This time, the DNA probes contained D-threoninol-based units with perylene and anthraquinone as a fluorophore and quencher, respectively (to promote quenching in the presence of the cell extract). The probes were sufficiently resistant to enzymatic degradation and showed sufficient affinity to reliably detect the target RNA in lysate and in live cells. An excellent signal-to-noise value of 1600 was observed for the 22-nt probe carrying four perylene and two anthraquinone moieties.

6. Serinol Nucleic Acids (SNA)

Compared to aTNA, the acyclic flexible scaffold of serinol nucleic acids (33, Chart 10, a dinucleotide is shown) does not contain a methyl group (in the position next to the amino group), which gives rise to the phenomenon of two stereogenic centers in the aTNA unit [68]. Thus, the chirality of the SNA molecule synthesized from four SNA monomers depends only on its sequence. The chirality of oligomers is denoted by (*R*) and (*S*) descriptors assigned to each end according to the chirality of the terminal residues. If the sequence is palindromic (e.g., ATTGCGTTA or pATTGCGTTAp), the entire molecule is achiral, although there is a carbon atom with four different substituents in each SNA unit except the central one. When an oligomer has an odd number of SNA units (e.g., ApTpTpGpCpGpTpTpA), the plane of symmetry passes through the central carbon atom

of the backbone within the central SNA unit, which is SNA-C in this example. When this number is even (e.g., ApTpTpGpGpTpTpA), the symmetry plane passes through the central phosphorus atom, which is marked as underlined. In both cases, these are the *meso* forms. When a sequence is non-palindromic (e.g., ATTGCGTAA, pATTGCGTTA or ATTGCGTTAp), the molecule is chiral.

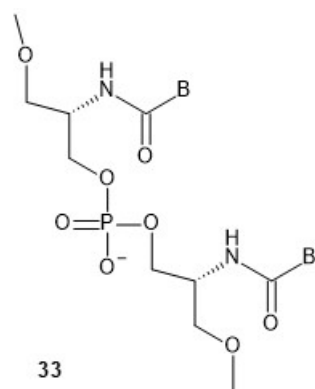
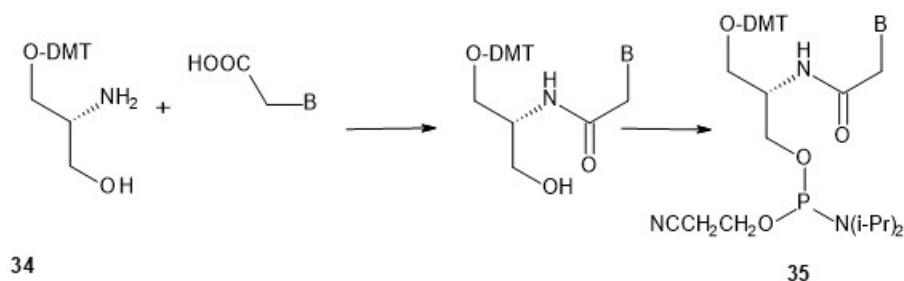


Chart 10. Structure of SNA dinucleotide.

Four chiral SNA-phosphoramidite monomers **35** were synthesized by condensation of the carboxymethyl derivatives of nucleobases (A^{Bz} , T, G^{iBu} or C^{Bz}) with the amino group of amino alcohol **34** (Scheme 7) obtained from L-serine. The procedure used for the synthesis of the DMT-protected amino alcohol [69] allowed to obtain enantiomerically pure compounds, which were used for the synthesis of seven SNA-octamers. Their combinations should yield chiral antiparallel, chiral parallel and achiral duplexes.



Scheme 7. Synthesis of the phosphoramidite monomers for synthesis of SNA.

In addition, DNA and RNA oligomers isosequential with the SNA oligomers were prepared, and the thermal stability of SNA, DNA and RNA homoduplexes, as well as SNA/DNA and SNA/RNA heteroduplexes, was determined. The melting experiments showed that not only were the expected antiparallel SNA homoduplexes formed ($T_m = 51\text{ }^\circ\text{C}$), but also the parallel ones, although the latter were much less stable ($T_m = 16\text{ }^\circ\text{C}$). Importantly, however, the antiparallel SNA/SNA duplexes were much more stable than the isosequential DNA/DNA ($T_m = 23$ or $29\text{ }^\circ\text{C}$) or RNA/RNA ($T_m = 38$ or $39\text{ }^\circ\text{C}$) complexes. It should be emphasized that SNA oligomers formed antiparallel heteroduplexes with DNA and RNA matrices whose stability was only a few degrees lower than that of the DNA/DNA (20–24 vs. 23–29 $^\circ\text{C}$) and RNA/RNA (32–36 vs. 38–39 $^\circ\text{C}$) homoduplexes. Analogously to the previously described L-aTNA/RNA duplex [59], a crystal structure showed that an SNA/RNA duplex adopts right-handed helicity and uses the Watson-Crick base-pairing.

Two pairs of the synthesized oligomers were of inverted sequences, so they constituted two pairs of enantiomeric species. They were designed to answer a question about the possible helicity of the corresponding enantiomeric duplexes. Indeed, the corresponding CD spectra showed exactly inverse signals, confirming the existence of right- and left-

handed helices, and the handedness depended on the sequences. The spectrum recorded for the symmetric achiral duplex showed no induced CD signals.

To increase the thermal stability of the SNA/RNA duplexes, the adenine moieties were replaced with 2,6-diaminopurine (D), which forms a D:U pair (**36**, Chart 11) with uracil with three hydrogen bonds [70].

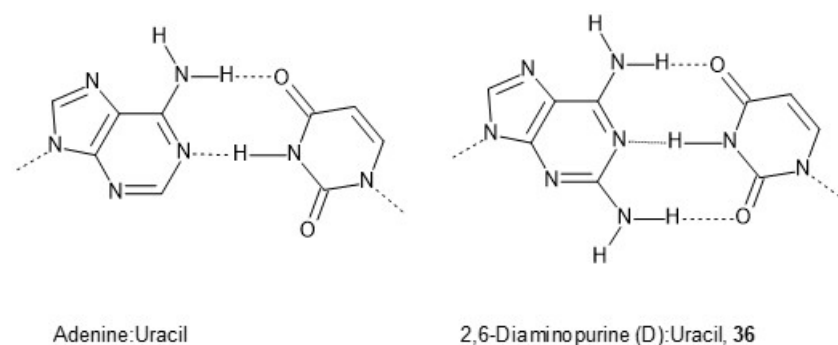
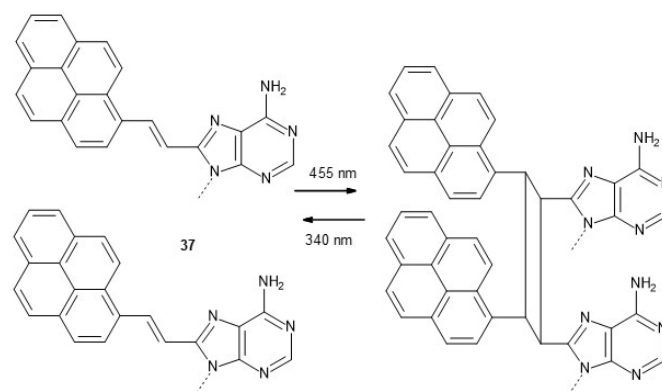


Chart 11. Hydrogen bonds in A:U and D:U base pairs.

While the melting experiment for a DNA/RNA duplex 5'-d(CAACATCAGTCTGAT AAGCTA)-3' / 5'-UAGCUUAUGAGACUGAUGUUG-3' yielded $T_m = 57\text{ }^\circ\text{C}$, this parameter increased to $67\text{ }^\circ\text{C}$ for the isosequential SNA/RNA duplex, and $T_m = 76\text{ }^\circ\text{C}$ was observed for the SNA/RNA analog in which CDDCDTCGCTGDTDDGCTA was the SNA component.

The above-mentioned strong stabilization of D:U or D:T base pairs may lead to an undesirable situation in which strong hydrogen bonds promote the formation of intramolecular double-stranded structures within an SNA probe, thereby interfering with hybridization with the target RNA. To avoid undesirable self-hybridization, SNA nucleotides carrying 2-thiothymine (T^S) or 2-thiouracil (U^S) instead of thymine or uracil have been developed [71]. The sulfur atom (which has a much larger atomic radius than an oxygen atom) at the C2 position causes a steric hindrance that prevents intramolecular pairing with the amino group at position 2 in 2,6-diaminopurine. On the other hand, the D residue in SNA interacts with T and U in a complementary DNA or RNA strand, respectively, and sulfur-substituted SNA- T^S and SNA- U^S normally hybridize with A in the target oligomer.

An interesting way to control the strength of SNA/RNA hybridization is based on the photochemically induced [2 + 2] cycloaddition of two 8-pyrenylvinyl adenine residues (**37**, Scheme 8) present in adjacent positions to each other in an SNA strand [72].



Scheme 8. Photochemically induced [2 + 2]-cycloaddition of two 8-pyrenylvinyl-adenine residues.

Such a modified adenine exerts the canonical Watson-Crick base-pairing with thymine or uracil. A model SNA oligomer of sequence GCTA*A*TGC, where the letter A* stands for 8-pyrenylvinyl-adenine, and an RNA oligomer 5'-AAGCAUUAGCAA-3 complementary to the underlined segment, form a duplex with $T_m = 35\text{ }^\circ\text{C}$. After irradiation with 455

nm light at 20 °C for 1 h, almost complete crosslinking was noted and no melting transition was observed, proving that the duplex was dissociated. The authors claim that the local structure around the crosslinked $A^*=A^*$ was disturbed to the extent that the dissociation of the duplex was forced. Upon irradiation with 340 nm light, 90% of the crosslinking was reversed within 15 min, and a sigmoidal melting curve was recorded. Importantly, three successive crosslinking/recovery processes were possible by alternating irradiation with 455 and 340 nm light without significant photobleaching.

Similar functionality was achieved with 8-naphthylvinyl-adenine (A^N , **38**, Chart 12), although in this case crosslinking to form the $A^N=A^N$ adduct was performed with light of 340–405 nm (455 nm for $A^*=A^*$) and the restoration of A^N occurred upon irradiation with ≤ 300 nm light (340 nm for A^*) [73]. For a system A^* , A^N crosslinking to $A^*=A^N$ was performed with light from 405 to 465 nm and recovery occurred upon irradiation with ≤ 340 nm. Since certain wavelength ranges for (A^* , A^N) and (A^N , A^N) do not overlap, it was possible to selectively generate four possible hybridization states using a mixture of SNA-(A^* , A^N) and SNA-(A^N , A^N). A suitable combination of wavelengths is: 340–405 nm to form $A^N=A^N$, 405–465 nm to form $A^*=A^N$, ≤ 300 nm to recover (A^N , A^N) and ≤ 340 nm to recover (A^* , A^N). The authors also found that SNA-(A^* , A^*) cannot be used in this double-switch because a simultaneous cyclo-reversion of $A^*=A^*$ and $A^N=A^N$ would be impossible due to the poor absorption of 300 nm light by the $A^*=A^*$ photo-adduct.

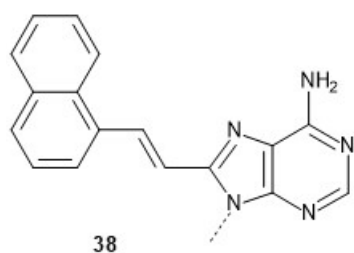


Chart 12. 8-naphthylvinyl-adenine.

SNA constructs are also used as analytical tools in biology and biochemistry. In a similar approach to the DNA probe using aTNA-erythrin units [66], a fluorescent 5-(peryleneethynyl)uracil unit (PeU) was incorporated into SNA molecules as a substitute for thymine [74]. In the single-stranded state, interactions between the perylenes resulted in self-quenching of the fluorophores. Upon hybridization with the target strand, the fluorophores intercalate, and the quenching does not occur, resulting in fluorescence emission at $\lambda \approx 490$ nm of the perylene molecules. Finally, a quencher-free linear SNA probe containing three PeU units, each separated by six nucleobases, was synthesized, allowing detection of target RNA with high sensitivity and discrimination of a single-base mismatch. The differences in fluorescence were visible to the naked eye, as the single strand had yellow emission, the fully matched duplex emitted bright green light and the mismatched duplex emitted faint green fluorescence.

The SNA scaffold has been successfully used to prepare molecular beacons (SNA-MB) bearing a fluorophore (perylene or Cy3) and the anthraquinone quencher at opposite ends [75]. Both fluorophore/quencher pairs worked well, and strong fluorescence emissions were observed for complementary target RNAs, almost equal to those of a single strand carrying only the fluorophore. A signal-to-noise ratio of up to 930 was observed for the perylene/anthraquinone pair. Fluorescence measurements in the lysate of HeLa cells showed that the SNA-MBs were resistant to degradation by nuclease and the probes could be used to visualize mRNA in fixed cells.

It was found that SNA-type nucleotides could enhance the efficacy of oligomers acting in the RNA interference process. In the dual luciferase assay, an siRNA duplex and its analogs modified with 1, 3, 5 or 7 SNA nucleotides at each of the sense strands or at the 3' end of the antisense strand were prepared [76]. PAGE Analysis of the products of incubation of siRNAs with cell lysate showed that the increasing number of SNA modifications led to

a deterioration of siRNA stability. For example, a duplex with seven modifications at each end of the passenger strand and at the 3'-end of the guide strand was largely hydrolyzed after only 1 min of incubation. Moreover, RNAi activity decreased with increasing number of SNA substitutions on the antisense strand. The authors conclude that substitutions of an SNA residue at each end of the passenger strand and at the 3'-end of the antisense strand were most effective, as they conferred the best resistance to nucleolytic degradation and virtually eliminated incorporation of the sense strand into the RISC complex without inhibiting silencing activity.

The aforementioned phenomenon that SNA molecules of palindromic sequences are achiral was the basis for the construction of a nanowire that functions as a helical amplification system [77]. The nanowires were formed by hybridizing the palindromic SNA oligomers (S)-TCGTCCTGCT-(R) and (R)-GACGAAGCAG-(S), which are partially complementary across the underlined segments. The duplexes possessed 5-nt overhangs—AGCAG-(S) and (S)-TCGTC—and used these to continue hybridization. Atomic force spectroscopy of the resulting nanowires revealed an average length of 53.6 nm. Melting analysis revealed $T_m = 46.7$ °C, indicating that the complex is stable at room temperature. The CD measurement performed for the fully complementary SNA duplex (S)-TCGTCCTGCT-(R)/(R)-AGCAGGACGA-(S), which should be achiral due to the palindromic sequence, showed only very weak signals, if any. The CD spectra changed completely when even small amounts (0.01 eq) of D-aTNA or L-aTNA oligomers 1'-TCGTCCTGCT-3' were added. The CD spectra had a negative peak at about 260 nm and a positive peak at about 285 nm, or a positive peak at 260 nm and a negative peak at 285 nm, respectively. Interestingly, the intensities increased with the number of equivalents of the given aTNA oligomer, but a plateau was reached after the addition of 0.2 equivalents. While amplitudes of 15 mdeg were detected in these experiments, the amplitudes of the CD signals increased linearly (no plateau) for the fully complementary duplex (S)-TCGTCCTGCT-(R)/(R)-AGCAGGACGA-(S) and did not exceed 6 mdeg. These different behaviors suggest that a nanostructure is required for helical amplification and that the helicity of the aTNAs was amplified by base stacks of the SNA nanowires. The authors suggest that the SNA nanowire system could be used to detect complementary DNA or RNA fragments, as SNA can recognize natural nucleic acids. Other biomolecules (proteins, sugars) could also be detected if these molecules could induce helicity in the SNA nanostructures.

7. Summary

The examples of acyclic nucleic acids presented in this review belong to six classes. Their synthesis is usually quite convenient (involving only a few steps) and there is usually the possibility of attaching fluorophores or other groups, e.g., photoactivated actuators or components suitable for cross-linking. Acyclic nucleic acids are attractive because of their remarkably high stability in body fluids. Of course, a negatively charged phosphate diester backbone poses a problem in crossing cell membranes, but on the other hand, it provides sufficient water solubility. Studies with fully modified oligomers have shown that, with few exceptions, their hybridization with natural DNA and RNA oligonucleotides generally works poorly or not at all. It is therefore questionable whether the next acyclic analogs can join the family of DNA/RNA analogs such as Peptide Nucleic Acids (PNA) or Locked Nucleic Acids (LNA), which form very stable duplexes with natural oligonucleotides. However, strong hybridization often leads to problems with selectivity. Therefore, the growing number of reports indicating that certain acyclic nucleotides help to achieve better specificity and higher stability of important and widely studied probes in the field of regulatory nucleic acids, e.g., in the RNAi method, is welcome. Highly specific fluorescent probes suitable for biochemical and biological studies have also been developed, as well as precisely activated “switches” with potential application in nanotechnology. Undoubtedly, new such constructs are under development. The range of acyclic nucleotides is expanding, and several other scaffolds have been used to prepare other analogs. For example, the synthesis of DiEthanol Amide Nucleic Acids (DEANA) has been published, in which the

nucleobases are attached to an achiral scaffold (with eight atoms in a unit) via amide bonds [78]. However, unlike GNA, TNA or SNA, DEANA homoduplexes are less stable than DNA duplexes of the same sequence. The same article describes the structurally very similar TriEthanol Amino Nucleic Acids (TEANA), which have the same scaffold as DEANA, but in which the bases are attached via an alkyl $-CH_2-CH_2-$ linker. However, unlike PNA, TNA, SNA or DEANA oligomers, the central nitrogen atom is not part of the amide group, so its protonation at physiological pH may lead to markedly different, not necessarily desirable or advantageous, properties. One can be sure that other scaffolds are currently being developed and new applications are being designed for them as well as for classes already under investigation.

Author Contributions: All author have contributed to the manuscript. All authors have read and agreed to the published version of the manuscript.

Funding: This work was financially supported by statutory funds of the Centre of Molecular and Macromolecular Studies, Polish Academy of Sciences, Łódź, Poland.

Conflicts of Interest: The authors declare no conflict of interest.

References

1. Leumann, C.J. DNA analogues: From supramolecular principles to biological properties. *Bioorg. Med. Chem.* **2002**, *10*, 841–854. [[CrossRef](#)]
2. Joyce, G.F.; Schwartz, A.W.; Miller, S.L.; Orgel, L.E. The case for an ancestral genetic system involving simple analogues of the nucleotides. *Proc. Natl. Acad. Sci. USA* **1987**, *84*, 4398–4440. [[CrossRef](#)] [[PubMed](#)]
3. Schneider, K.C.; Benner, S.A. Oligonucleotides containing flexible nucleoside analogs. *J. Am. Chem. Soc.* **1990**, *112*, 453–455. [[CrossRef](#)]
4. Merle, Y.; Bonneil, E.; Merle, L.; Saggi, J.; Szemzo, A. Acyclic oligonucleotide analogues. *Int. J. Biol. Macromol.* **1995**, *17*, 239–246. [[CrossRef](#)]
5. Chaput, J.C.; Switzer, C. Nonenzymatic oligomerization on templates containing phosphodiester-linked acyclic glycerol nucleic acid analogues. *J. Mol. Evol.* **2000**, *51*, 464–470. [[CrossRef](#)] [[PubMed](#)]
6. Nielsen, P.; Dreier, L.H.; Wengel, J. Synthesis and evaluation of oligodeoxynucleotides containing acyclic nucleosides: Introduction of three novel analogues and a summary. *Bioorg. Med. Chem.* **1995**, *3*, 19–28. [[CrossRef](#)]
7. Langkjær, N.; Pasternak, A.; Wengel, J. UNA (unlocked nucleic acid): A flexible RNA mimic that allows engineering of nucleic acid duplex stability. *Bioorg. Med. Chem.* **2009**, *17*, 5420–5425. [[CrossRef](#)] [[PubMed](#)]
8. Mangos, M.M.; Min, K.-L.; Viazovkina, E.; Galarneau, A.; Elzagheid, M.J.; Parniak, M.A.; Damha, M.J. Efficient RNase H-directed cleavage of RNA promoted by antisense DNA or 2′F-ANA constructs containing acyclic nucleotide inserts. *J. Am. Chem. Soc.* **2003**, *125*, 654–661. [[CrossRef](#)]
9. Singh, S.K.; Chandrashekar Reddy, L.; Srivastava, S.; Olsen, C.E.; Sanghvi, Y.S.; Langkjær, N.; Wengel, J.; Parmar, V.S.; Prasad, A.K. Selective biocatalytic acylation studies on 5′-O-(4,4′-dimethoxytrityl)-2′,3′-secouridine: An efficient synthesis of UNA monomer. *Nucleosides Nucleotides Nucleic Acids* **2012**, *31*, 831–840. [[CrossRef](#)]
10. Jensen, T.B.; Langkjær, N.; Wengel, J. Unlocked nucleic acid (UNA) and UNA derivatives: Thermal denaturation studies. *Nucleic Acids Symp. Ser.* **2008**, *52*, 133–134. [[CrossRef](#)]
11. Robertson, N.M.; Toscano, A.E.; LaMantia, V.E.; Salih Hizir, M.; Rana, M.; Balcioglu, M.; Sheng, J.; Yigit, M.V. Unlocked Nucleic Acids for miRNA detection using two dimensional nano-graphene oxide. *Biosens. Bioelectron.* **2017**, *89*, 551–557. [[CrossRef](#)]
12. Pasternak, A.; Wengel, J. Thermodynamics of RNA duplexes modified with unlocked nucleic acid nucleotides. *Nucleic Acids Res.* **2010**, *38*, 6697–6706. [[CrossRef](#)] [[PubMed](#)]
13. Guéron, M.; Leroy, J.-L. The *i*-motif in nucleic acids. *Curr. Opin. Struct. Biol.* **2000**, *10*, 326–331. [[CrossRef](#)]
14. Pasternak, A.; Wengel, J. Modulation of *i*-motif thermodynamic stability by the introduction of UNA (unlocked nucleic acid) monomers. *Bioorg. Med. Chem. Lett.* **2011**, *21*, 752–755. [[CrossRef](#)] [[PubMed](#)]
15. Agarwal, T.; Kumar, S.; Maiti, S. Unlocking G-quadruplex: Effect of unlocked nucleic acid on G-quadruplex stability. *Biochimie* **2011**, *93*, 1694–1700. [[CrossRef](#)]
16. Pasternak, A.; Hernandez, F.J.; Rasmussen, L.M.; Vester, B.; Wengel, J. Improved thrombin binding aptamer by incorporation of a single unlocked nucleic acid monomer. *Nucleic Acids Res.* **2011**, *39*, 1155–1164. [[CrossRef](#)]
17. Jensen, T.B.; Henriksen, J.R.; Rasmussen, B.E.; Rasmussen, L.M.; Andresen, T.L.; Wengel, J.; Pasternak, A. Thermodynamic and biological evaluation of a thrombin binding aptamer modified with several unlocked nucleic acid (UNA) monomers and a 2′-C-piperazino-UNA monomer. *Bioorg. Med. Chem.* **2011**, *19*, 4739–4745. [[CrossRef](#)] [[PubMed](#)]
18. Kotkowiak, W.; Lisowiec-Wachnicka, J.; Grynda, J.; Kierzek, R.; Wengel, J.; Pasternak, A. Thermodynamic, Anticoagulant, and Antiproliferative Properties of Thrombin Binding Aptamer Containing Novel UNA Derivative. *Mol. Ther. Nucleic Acids* **2018**, *10*, 304–316. [[CrossRef](#)]

19. Aaldering, L.J.; Poongavanam, V.; Langkjær, N.; Murugan, N.A.; Jørgensen, P.T.; Wengel, J.; Veedu, R.N. Development of an Efficient G-Quadruplex-Stabilised Thrombin-Binding Aptamer Containing a Three-Carbon Spacer Molecule. *ChemBioChem* **2017**, *18*, 755–763. [[CrossRef](#)]
20. Nallagatla, S.R.; Heuberger, B.; Haque, A.; Switzer, C. Combinatorial synthesis of thrombin-binding aptamers containing iso-guanine. *J. Comb. Chem.* **2009**, *11*, 364–369. [[CrossRef](#)]
21. Kotkowiak, W.; Czapik, T.; Pasternak, A. Novel isoguanine derivative of unlocked nucleic acid—Investigations of thermodynamics and biological potential of modified thrombin binding aptamer. *PLoS ONE* **2018**, *13*, e0197835. [[CrossRef](#)]
22. Mazurov, A.V.; Titaeva, E.V.; Khaspekova, S.G.; Storozhilova, A.N.; Spiridonova, V.A.; Kopylov, A.M.; Dobrovolsky, A.B. Characteristics of a new DNA aptamer, direct inhibitor of thrombin. *Bull. Exp. Biol. Med.* **2011**, *150*, 422–425. [[CrossRef](#)]
23. Kotkowiak, W.; Wengel, J.; Scotton, C.J.; Pasternak, A. Improved RE31 Analogues Containing Modified Nucleic Acid Monomers: Thermodynamic, Structural, and Biological Effects. *J. Med. Chem.* **2019**, *62*, 2499–2507. [[CrossRef](#)]
24. Laursen, M.B.; Pakula, M.M.; Gao, S.; Fluiter, K.; Mook, O.R.; Baas, F.; Langklær, N.; Wengel, S.L.; Wengel, J.; Kjemsab, J.; et al. Utilization of unlocked nucleic acid (UNA) to enhance siRNA performance in vitro and in vivo. *Mol. BioSyst.* **2010**, *6*, 862–870. [[CrossRef](#)] [[PubMed](#)]
25. Kenski, D.M.; Cooper, A.J.; Li, J.J.; Willingham, A.T.; Haringsma, H.J.; Young, T.A.; Kuklin, N.A.; Jones, J.J.; Cancilla, M.T.; McMasters, D.R.; et al. Analysis of acyclic nucleoside modifications in siRNAs finds sensitivity at position 1 that is restored by 5'-terminal phosphorylation both in vitro and in vivo. *Nucleic Acids Res.* **2010**, *38*, 660–671. [[CrossRef](#)]
26. Bramsen, J.B.; Pakula, M.M.; Hansen, T.B.; Bus, C.; Langkjær, N.; Odadzic, D.; Smicius, R.; Wengel, S.L.; Chattopadhyaya, J.; Engels, J.W.; et al. A screen of chemical modifications identifies position-specific modification by UNA to most potently reduce siRNA off-target effects. *Nucleic Acids Res.* **2010**, *38*, 5761–5773. [[CrossRef](#)] [[PubMed](#)]
27. Werk, D.; Wengel, J.; Wengel, S.L.; Grunert, H.-P.; Zeichhardt, H.; Kurreck, J. Application of small interfering RNAs modified by unlocked nucleic acid (UNA) to inhibit the heart-pathogenic coxsackievirus B3. *FEBS Lett.* **2010**, *584*, 591–598. [[CrossRef](#)] [[PubMed](#)]
28. Vaish, N.; Chen, F.; Seth, S.; Fosnaugh, K.; Liu, Y.; Adami, R.; Brown, T.; Chen, Y.; Harvie, P.; Johns, R.; et al. Improved specificity of gene silencing by siRNAs containing unlocked nucleobase analogs. *Nucleic Acids Res.* **2011**, *39*, 1823–1832. [[CrossRef](#)]
29. Karlsen, K.K.; Pasternak, A.; Jensen, T.B.; Wengel, J. Pyrene-modified unlocked nucleic acids: Synthesis, thermodynamic studies, and fluorescent properties. *ChemBioChem* **2012**, *13*, 590–601. [[CrossRef](#)] [[PubMed](#)]
30. Karlsen, K.K.; Okholm, A.; Kjems, J.; Wengel, J. A quencher-free molecular beacon design based on pyrene excimer fluorescence using pyrene-labeled UNA (unlocked nucleic acid). *Bioorg. Med. Chem.* **2013**, *21*, 6186–6190. [[CrossRef](#)]
31. Perlikova, P.; Karlsen, K.K.; Pedersen, E.B.; Wengel, J. Unlocked nucleic acids with a pyrene-modified uracil: Synthesis, hybridization studies, fluorescent properties and i-motif stability. *ChemBioChem* **2014**, *15*, 146–156. [[CrossRef](#)]
32. Perlikova, P.; Ejlersen, M.; Langkjær, N.; Wengel, J. Bis-pyrene-modified unlocked nucleic acids: Synthesis, hybridization studies, and fluorescent properties. *ChemMedChem* **2014**, *9*, 2120–2127. [[CrossRef](#)] [[PubMed](#)]
33. Ejlersen, M.; Langkjær, N.; Wengel, J. 3'-Pyrene-modified unlocked nucleic acids: Synthesis, fluorescence properties and a surprising stabilization effect on duplexes and triplexes. *Org. Biomol. Chem.* **2017**, *15*, 2073–2085. [[CrossRef](#)] [[PubMed](#)]
34. Zhang, L.; Peritz, A.; Meggers, E. A simple glycol nucleic acid. *J. Am. Chem. Soc.* **2005**, *127*, 4174–4175. [[CrossRef](#)] [[PubMed](#)]
35. Zhang, L.; Peritz, A.E.; Carroll, P.J.; Meggers, E. Synthesis of Glycol Nucleic Acids. *Synthesis* **2006**, 645–653.
36. Schlegel, M.K.; Meggers, E. Improved phosphoramidite building blocks for the synthesis of the simplified nucleic acid GNA. *J. Org. Chem.* **2009**, *74*, 4615–4618. [[CrossRef](#)]
37. Schlegel, M.K.; Peritz, A.E.; Kittigowittana, K.; Zhang, L.; Meggers, E. Duplex formation of the simplified nucleic acid GNA. *ChemBioChem* **2007**, *8*, 927–932. [[CrossRef](#)]
38. Schlegel, M.K.; Xie, X.; Zhang, L.; Meggers, E. Insight into the high duplex stability of the simplified nucleic acid GNA. *Angew. Chem. Int. Ed.* **2009**, *48*, 960–963. [[CrossRef](#)]
39. Schlegel, M.K.; Essen, L.-O.; Meggers, E. Duplex structure of a minimal nucleic acid. *J. Am. Chem. Soc.* **2008**, *130*, 8158–8159. [[CrossRef](#)]
40. Schlegel, M.K.; Essen, L.-O.; Meggers, E. Atomic resolution duplex structure of the simplified nucleic acid GNA. *Chem. Commun.* **2010**, *46*, 1094–1096. [[CrossRef](#)]
41. Johnson, A.T.; Schlegel, M.K.; Meggers, E.; Essen, L.-O.; Wiest, O. On the structure and dynamics of duplex GNA. *J. Org. Chem.* **2011**, *76*, 7964–7974. [[CrossRef](#)]
42. Tsai, C.-H.; Chen, J.; Szostak, J.W. Enzymatic synthesis of DNA on glycerol nucleic acid templates without stable duplex formation between product and template. *Proc. Natl. Acad. Sci. USA* **2007**, *104*, 14598–14603. [[CrossRef](#)]
43. Chen, J.J.; Tsai, C.-H.; Cai, X.; Horhota, A.T.; McLaughlin, L.W.; Szostak, J.W. Enzymatic primer-extension with glycerol-nucleoside triphosphates on DNA templates. *PLoS ONE* **2009**, *4*, e4949. [[CrossRef](#)]
44. Aviñó, A.; Mazzini, S.; Fàbrega, C.; Peñalver, P.; Gargallo, R.; Morales, J.C.; Eritja, R. The effect of 1-thymidine, acyclic thymine and 8-bromoguanine on the stability of model G-quadruplex structures. *Biochim. Biophys. Acta* **2017**, *1861*, 1205–1212. [[CrossRef](#)] [[PubMed](#)]
45. Schlegel, M.K.; Foster, D.J.; Kel'in, A.V.; Zlatev, I.; Bisbe, A.; Jayaraman, M.; Lackey, J.G.; Rajeev, K.G.; Charissé, K.; Harp, J.; et al. Chirality Dependent Potency Enhancement and Structural Impact of Glycol Nucleic Acid Modification on siRNA. *J. Am. Chem. Soc.* **2017**, *139*, 8537–8546. [[CrossRef](#)] [[PubMed](#)]

46. Coantic-Castex, S.; Martinez, A.; Harakat, D.; Guillaume, D.; Clivi, P. The remarkable UV light invulnerability of thymine GNA dinucleotides. *Chem. Commun.* **2019**, *55*, 12571–12574. [[CrossRef](#)]
47. Zhang, R.S.; McCullum, E.O.; Chaput, J.C. Synthesis of Two Mirror Image 4-Helix Junctions Derived from Glycerol Nucleic Acid. *J. Am. Chem. Soc.* **2008**, *130*, 5846–5847. [[CrossRef](#)]
48. Schlegel, M.K.; Zhang, L.; Pagano, N.; Meggers, E. Metal-mediated base pairing within the simplified nucleic acid GNA. *Org. Biomol. Chem.* **2009**, *7*, 476–482. [[CrossRef](#)]
49. Zhou, H.; Johnson, A.T.; Wiest, O.; Zhang, L. Incorporation of porphyrin acetylides into duplexes of the simplified nucleic acid GNA. *Org. Biomol. Chem.* **2011**, *9*, 2840–2849. [[CrossRef](#)]
50. Xiang, Y.; Zhang, Q.; Li, Z.; Chen, H. Role of electrostatic complementarity between perylene diimide and porphyrin in highly stabilized GNA. *Mater. Sci. Eng. C Mater. Biol. Appl.* **2017**, *70*, 1156–1162. [[CrossRef](#)]
51. Jash, B.; Müller, J. Stable Copper (I)—Mediated Base Pairing in DNA. *Angew. Chem. Int. Ed.* **2018**, *57*, 9524–9527. [[CrossRef](#)]
52. Jash, B.; Müller, J. A stable zinc (II)—Mediated base pair in a parallel-stranded DNA duplex. *J. Inorg. Biochem.* **2018**, *186*, 301–306. [[CrossRef](#)] [[PubMed](#)]
53. Jash, B.; Müller, J. Concomitant Site-Specific Incorporation of Silver (I) and Mercury (II) Ions into a DNA Duplex. *Chem. Eur. J.* **2018**, *24*, 10636–10640. [[CrossRef](#)]
54. Jash, B.; Müller, J. Stable Hg (II)—Mediated base pairs with a phenanthroline-derived nucleobase surrogate in antiparallel-stranded DNA. *J. Biol. Inorg. Chem.* **2020**, *25*, 647–654. [[CrossRef](#)] [[PubMed](#)]
55. Piotrowicz, M.; Kowalczyk, A.; Trzybiński, D.; Woźniak, K.; Kowalski, K. Redox-Active Glycol Nucleic Acid (GNA) Components: Synthesis and Properties of the Ferrocenyl-GNA Nucleoside, Phosphoramidite, and Semicanonical Dinucleoside Phosphate. *Organometallics* **2020**, *39*, 813–823. [[CrossRef](#)]
56. Kumar, V.; Gore, K.R.; Pradeepkumar, P.I.; Kesavan, V. Design, synthesis, biophysical and primer extension studies of novel acyclic butyl nucleic acid (BuNA). *Org. Biomol. Chem.* **2013**, *11*, 5853–5865. [[CrossRef](#)]
57. Asanuma, H.; Toda, T.; Murayama, K.; Liang, X.; Kashida, H. Unexpectedly Stable Artificial Duplex from Flexible Acyclic Threoninol. *J. Am. Chem. Soc.* **2010**, *132*, 14702–14703. [[CrossRef](#)]
58. Murayama, K.; Kashida, H.; Asanuma, H. Acyclic L-threoninol nucleic acid (L-aTNA) with suitable structural rigidity cross-pairs with DNA and RNA. *Chem. Commun.* **2015**, *51*, 6500–6503. [[CrossRef](#)]
59. Kamiya, Y.; Slatoh, T.; Kodama, A.; Suzuki, T.; Murayama, K.; Kashida, H.; Uchiyama, S.; Kato, K.; Asanuma, H. Intrastrand backbone-nucleobase interactions stabilize unwound right-handed helical structures of heteroduplexes of L-aTNA/RNA and SNA/RNA. *Commun. Chem.* **2020**, *3*, 156. [[CrossRef](#)]
60. Kumar, V.; Kesavan, V.; Gothelf, K.V. Highly stable triple helix formation by homopyrimidine (L)-acyclic threoninol nucleic acids with single stranded DNA and RNA. *Org. Biomol. Chem.* **2015**, *13*, 2366–2374. [[CrossRef](#)]
61. Nguyen, T.J.D.; Manuguerra, I.; Kumar, V.; Gothelf, K.V. Toehold-Mediated Strand Displacement in a Triplex Forming Nucleic Acid Clamp for Reversible Regulation of Polymerase Activity and Protein Expression. *Chem. Eur. J.* **2019**, *25*, 12303–12307. [[CrossRef](#)] [[PubMed](#)]
62. Kumar, V.; Gothel, K.V. Synthesis and biophysical properties of (L)-aTNA based G-quadruplexes. *Org. Biomol. Chem.* **2016**, *14*, 1540–1544. [[CrossRef](#)]
63. Kumar, V.; Nguyen, T.J.D.; Palmfeldt, J.; Gothelf, K.V. Formation of *i*-motifs from acyclic (L)-threoninol nucleic acids. *Org. Biomol. Chem.* **2019**, *17*, 7655–7659. [[CrossRef](#)]
64. Alagia, A.; Terrazas, M.; Eritja, R. RNA/aTNA Chimeras: RNAi Effects and Nucleases Resistance of Single and Double Stranded RNAs. *Molecules* **2014**, *19*, 17872–17896. [[CrossRef](#)]
65. Alagia, A.; Terrazas, M.; Eritja, R. Modulation of the RNA Interference Activity Using Central Mismatched siRNAs and Acyclic Threoninol Nucleic Acids (aTNA) Units. *Molecules* **2015**, *20*, 7602–7619. [[CrossRef](#)]
66. Asanuma, H.; Akahane, M.; Kondo, N.; Osawa, T.; Kato, T.; Kashida, H. Quencher-free linear probe with multiple fluorophores on an acyclic scaffold. *Chem. Sci.* **2012**, *3*, 3165–3169. [[CrossRef](#)]
67. Asanuma, H.; Akahane, M.; Niwa, R.; Kashida, H.; Kamiya, Y. Highly Sensitive and Robust Linear Probe for Detection of mRNA in Cells. *Angew. Chem. Int. Ed.* **2015**, *54*, 4315–4319. [[CrossRef](#)]
68. Kashida, H.; Murayama, K.; Toda, T.; Asanuma, H. Control of the Chirality and Helicity of Oligomers of Serinol Nucleic Acid (SNA) by Sequence Design. *Angew. Chem. Int. Ed.* **2011**, *50*, 1285–1288. [[CrossRef](#)] [[PubMed](#)]
69. Benhida, R.; Devys, M.; Fourrey, J.-L.; Lecubin, F.; Sun, J.-S. Incorporation of serinol derived acyclic nucleoside analogues into oligonucleotides: Influence on duplex and triplex formation. *Tetrahedron Lett.* **1998**, *39*, 6167–6170. [[CrossRef](#)]
70. Kamiya, Y.; Donoshita, Y.; Kamimoto, H.; Murayama, K.; Ariyoshi, J.; Asanuma, H. Introduction of 2,6-Diaminopurines into Serinol Nucleic Acid Improves Anti-miRNA Performance. *ChemBioChem* **2017**, *18*, 1917–1922. [[CrossRef](#)] [[PubMed](#)]
71. Kamiya, Y.; Sato, F.; Murayama, K.; Kodama, A.; Uchiyama, S.; Asanuma, H. Incorporation of Pseudo-complementary Bases 2,6-Diaminopurine and 2-Thiouracil into Serinol Nucleic Acid (SNA) to Promote SNA/RNA Hybridization. *Chem. Asian J.* **2020**, *15*, 1266–1271. [[CrossRef](#)]
72. Murayama, K.; Yamano, Y.; Asanuma, H. 8-Pyrenylvinyl Adenine Controls Reversible Duplex Formation between Serinol Nucleic Acid and RNA by [2 + 2] Photocycloaddition. *J. Am. Chem. Soc.* **2019**, *141*, 9485–9489. [[CrossRef](#)] [[PubMed](#)]
73. Yamano, Y.; Murayama, K.; Asanuma, H. Dual Crosslinking Photo-Switches for Orthogonal Photo-Control of Hybridization Between Serinol Nucleic Acid and RNA. *Chem. Eur. J.* **2021**, *27*, 4599–4604. [[CrossRef](#)]

74. Murayama, K.; Asanuma, H. A Quencher-Free Linear Probe from Serinol Nucleic Acid with a Fluorescent Uracil Analogue. *ChemBioChem* **2020**, *21*, 120–128. [[CrossRef](#)] [[PubMed](#)]
75. Murayama, K.; Kamiya, Y.; Kashida, H.; Asanuma, H. Ultrasensitive Molecular Beacon Designed with Totally Serinol Nucleic Acid (SNA) for Monitoring mRNA in Cells. *ChemBioChem* **2015**, *16*, 1298–1301. [[CrossRef](#)]
76. Kamiy, Y.; Takai, J.; Ito, H.; Murayama, K.; Kashida, H.; Asanuma, H. Enhancement of Stability and Activity of siRNA by Terminal Substitution with Serinol Nucleic Acid (SNA). *ChemBioChem* **2014**, *15*, 2549–2555. [[CrossRef](#)]
77. Kashida, H.; Nishikawa, K.; Shi, W.; Miyagawa, T.; Yamashita, H.; Abe, M.; Asanuma, H. A helical amplification system composed of artificial nucleic acids. *Chem. Sci.* **2021**, *12*, 1656–1660. [[CrossRef](#)] [[PubMed](#)]
78. Srivastava, P.; El Asrar, R.A.; Knies, C.; Abramov, M.; Froeyen, M.; Rozenski, J.; Rosemeyer, H.; Herdewijn, P. Achiral, acyclic nucleic acids: Synthesis and biophysical studies of a possible prebiotic polymer. *Org. Biomol. Chem.* **2015**, *13*, 9249–9260. [[CrossRef](#)] [[PubMed](#)]